

Quantum-jumps and photon-statistic in fluorescent systems coupled to classically fluctuating reservoirs

Adrián A. Budini

*Consejo Nacional de Investigaciones Científicas y Técnicas,
Centro Atómico Bariloche, Avenida E. Bustillo Km 9.5, (8400) Bariloche, Argentina*
(Dated: May 21, 2010)

In this paper, we develop a quantum-jump approach for describing the photon-emission process of single fluorophore systems coupled to complex classically fluctuating reservoirs. The formalism relies on an open quantum system approach where the dynamic of the system and the reservoir fluctuations are described through a density matrix whose evolution is defined by a Lindblad rate equation. For each realization of the photon measurement processes it is possible to define a conditional system state (stochastic density matrix) whose evolution depends on both the photon detection events and the fluctuations between the configurational states of the reservoir. In contrast to standard fluorescent systems the photon-to-photon emission process is not a renewal one, being defined by a (stochastic) waiting time distribution that in each recording event parametrically depends on the conditional state. The formalism allows calculating experimental observables such as the full hierarchy of joint probabilities associated to the time intervals between consecutive photon recording events. These results provide a powerful basis for characterizing different situations arising in single-molecule spectroscopy, such as spectral fluctuations, lifetime fluctuations, and light assisted processes.

PACS numbers: 42.50.Lc, 42.50.Ct, 42.50.Ar, 33.80.-b

I. INTRODUCTION

A powerful theoretical formalism called the quantum-jump approach [1–11] was introduced by the quantum optics community for describing experimental realizations of single open quantum systems subjected to a continuous measurement process. Even when only one system is under observation, the quantum-jump approach allows to define a system state (wave vector or density matrix), whose dynamic takes into account our change of information due to the continuous measurement action. Apart from new insights in the quantum measurement theory, the quantum-jump approach provides an alternative formalism for characterizing the radiation pattern of single fluorescent systems driven by a laser field.

While a wide class of quantum optical systems can be studied with the quantum-jump approach [1–3], it has been scarcely applied in the context of single-molecule (fluorescence) spectroscopy (SMS) [12–14], i.e., in the characterization of single fluorescent systems coupled to complex host classically fluctuating environments, such as of those associated to biological or artificially designed nanoscopic reservoirs. The main task of SMS is to deduce the underlying environment stochastic dynamic from the statistical properties of the scattered laser field [15–25]. In most of the experiments, the scattered electromagnetic field is measured with photon detectors. Hence, it can be resolved photon-to-photon.

For direct photon-detection measurement schemes the quantum-jump approach associate to each photon recording event a sudden disruptive change (wave vector collapse) in the system state, while in the middle intervals between consecutive events the conditional-system evolution is smooth and non-unitary [1–6]. The formalism

provides a simple technique for calculating and reproducing the photon recording process. For Markovian dissipative dynamics the emission process is a *renewal* one, i.e., the statistic of the (random) time intervals between consecutive photon emissions is always the same, being defined by a probability distribution called waiting time distribution [1, 5].

The main obstacle for applying the quantum-jump approach for modeling SMS experiments comes from the description of the environment fluctuations. As in general a full microscopic description is lacking, the complexity of the environment is taken into account by introducing effective time-dependent stochastic variables that may modify (parametrize) both the unitary and dissipative fluorophore evolution. In the context of the quantum-jump approach, it is not clear how these extra (classical) fluctuations must to be introduced or consistently interpreted in terms of a continuous measurement action.

On the basis of stochastic models, the formalism of generalized Bloch equations [26–30] allows to determining the photon counting probabilities, i.e., the probabilities of detecting n -photons up to a given time. Nevertheless, from that approach it is not easy to know how the renewal property is broken by the external fluctuations, neither is known which kind of stochastic dynamic may reproduce the photon emission process. Then, objects like the hierarchy of joint probabilities associated to the time intervals between consecutive photon detections events is also unknown. These statistical objects can be obtained, for example, from a time average along a single measurement trajectory [see Eqs. (10) and (11)].

The main goal of this paper is to demonstrate that SMS experiments can be consistently described in the context of a quantum-jump approach. A general for-

malism that allows to characterize the photon-to-photon emission process for a broad class of environment fluctuations arising in SMS is developed. In each case, we provide (non-renewal) stochastic processes that reproduce the statistic of the photon recording events. The average of their associated dynamic in the system-bath Hilbert space recover the density matrix evolution. As a central result, we get explicit analytical expressions for the set of joint probabilities densities defining the statistics of the time intervals between successive photon recording events. Therefore, our analysis allows to quantify how and how much the photon emission process departs from a renewal one.

The formulation of an alternative description of SMS experiments based on a quantum-jump approach relies on the possibility of describing both the fluorophore and the environment fluctuations through a density matrix formalism. In Ref. [31] it was demonstrated that a broad class of SMS experiments can be studied through an open quantum system approach. The density matrix evolution is given by a Lindblad rate equation [32], which allows to characterize in a unified way both the quantum nature of the fluorescent system as well as the classical nature of the environment fluctuations. Based on those results, which are consistent [31] with the formalism of stochastic Bloch equations [26–30], we formulate the present treatment.

We remark that a similar analysis was developed in Ref. [33]. In contrast, our present analysis allows getting explicit expressions for the photon emission statistic, which is also analyzed in the limit of slow and fast environment fluctuations. Furthermore, an explicit formulation of the underlying stochastic photon emission process is presented. On the other hand, our results also clarifies some of the assumptions introduced in previous author's works [34–36] as well as in other stretched related contributions [37].

The paper is outlined as follows. In Sec. II, on the basis of the results developed in Ref. [31], we define the underlying density matrix formulation. In Sec. III, we develop the quantum-jump approach. Both, the stochastic dynamic and the statistical characterization of the photon emission process are established. In Sec. IV we apply the formalism for the case in which the measurement apparatus only gives information about the photon emission events. Different specific cases, such as lifetime fluctuations and light assisted processes, are analyzed in detail. In Appendix A we analyze the case of measurements that provide information of both the photon recording events and about the configurational reservoir transitions. In Sec. V we provide the conclusions.

II. DENSITY MATRIX EVOLUTION

The description of SMS experiments based on a density matrix formalism relies on the possibility of finding analytically manageable microscopic interactions able to

describe the environment fluctuations as well as their dynamical influence over the system. In Ref. [31], following an argument developed by van Kampen [38], we modeled the environment through a set of (effective, coarse grained) macrostates, each one representing the manifold of quantum bath states that lead to the same system dynamic. Then, the total microscopic dynamic is written in an effective Hilbert space defined by the external product of the Hilbert spaces of the system, the background electromagnetic field, and the configurational space associated to the bath macrostates. The system is modeled by a two-level optical transition whose characteristic parameters, i.e., transition frequency and electric dipole, depend on the state of the environment. The dielectric constant of its local environment also is parametrized by the bath macrostates. After tracing out the electromagnetic field and the configurational states, the density matrix $\rho_S(t)$ of the system can be written as [31]

$$\rho_S(t) = \sum_{R=1}^{R_{\max}} \rho_R(t). \quad (1)$$

Each auxiliary state $\rho_R(t)$ define the system dynamic *given* that the reservoir is in the R -configurational bath state. R_{\max} is the number of configurational states. The probability $P_R(t)$ that the environment is in a given state at time t follows from

$$P_R(t) = \text{Tr}_S[\rho_R(t)], \quad (2)$$

where $\text{Tr}_S[\dots]$ denotes a trace operation in the system Hilbert space. Therefore, the set of states $\{\rho_R(t)\}$ encode both the system dynamic and the fluctuations of the environment. Their dynamic is defined by a Lindblad rate equation [32]

$$\begin{aligned} \frac{d\rho_R(t)}{dt} = & \frac{-i}{\hbar} [H_R, \rho_R(t)] - \gamma_R(\{D, \rho_R(t)\}_+ - \mathcal{J}[\rho_R(t)]) \\ & - \sum_{\substack{R' \\ R' \neq R}} \frac{\eta_{R'R}}{2} \{A^\dagger A, \rho_R(t)\}_+ + \sum_{\substack{R' \\ R' \neq R}} \eta_{RR'} A \rho_{R'}(t) A^\dagger. \end{aligned} \quad (3)$$

The first line of this equation define the unitary and dissipative system dynamic given that the bath is in the configurational state R . The Hamiltonian H_R reads

$$H_R = \frac{\hbar\omega_R}{2} \sigma_z + \frac{\hbar\Omega_R}{2} (\sigma^\dagger e^{-i\omega_L t} + \sigma e^{i\omega_L t}), \quad (4)$$

where

$$\omega_R = (\omega_0 + \delta\omega_R). \quad (5)$$

The upper and lower states of the system are denoted as $|+\rangle$ and $|-\rangle$ respectively. Its transition frequency is ω_0 . σ_z is the z-Pauli matrix in the basis $\{|+\rangle, |-\rangle\}$. Then, the contribution $\hbar\omega_0\sigma_z/2$ defines the bare system Hamiltonian. The constants $\{\delta\omega_R\}$ define the spectral shifts associated to each bath state. The second contribution in Eq. (4) introduces the interaction between the system and the external laser excitation, whose frequency is ω_L .

The operators $\sigma^\dagger = |+\rangle\langle -|$ and $\sigma = |- \rangle\langle +|$ are the raising and lowering operators acting on system eigenstates. The Rabi frequencies $\{\Omega_R\}$ measure the strength of the system-laser coupling for each configurational bath state. The rest of the system operators appearing in Eq. (3) are defined by

$$D = \sigma^\dagger \sigma / 2, \quad \mathcal{J}[\bullet] = \sigma \bullet \sigma^\dagger, \quad (6)$$

while $\{\dots\}_+$ denotes an anticommutation operation. Then, the contribution proportional to the constant γ_R defines the natural decay of the system associated to each reservoir state.

The second line in Eq. (3) introduces a coupling (with rates $\eta_{R'R}$) between all the states $\{\rho_R(t)\}$, representing the fluctuations (transitions) between the configurational states of the environment. Depending on the definition of the system operator A different cases are recovered. When $A = I$, where I is the identity operator, the transitions between the configurational states do not depend on the system state. Hence, the probabilities (2) are governed by a classical master equation whose structure follows straightforwardly from Eq. (3). This case allows us to describe situations such as spectral diffusion processes, conformational environment fluctuations that affect the natural decay of the system, as well as single fluorophore systems diffusing in a solution [31]. When $A \neq I$, the configurational fluctuations are statistically entangled with the state of the system. Depending on the structure of A different kind of situations can be described such as for example light assisted process, where the fluctuations of the bath depend on the external laser field intensity.

Vectorial representation

In order to establish a general formulation of the quantum-jump approach, we introduce a vectorial notation that allow to simplifying the presentation and calculations. To the configurational bath states we associate a vectorial space, defined by a basis $\{|R\rangle\}_{R=1}^{R_{\max}}$, with $\langle R|R'\rangle = \delta_{RR'}$, each vector $|R\rangle$ being related to a different configurational bath state [39]. The set of auxiliary states $\{\rho_R(t)\}$ allows us to define the vectors

$$|\rho_t\rangle \equiv \sum_R \rho_R(t) |R\rangle, \quad |P_t\rangle \equiv \sum_R \text{Tr}_S[\rho_R(t)] |R\rangle. \quad (7)$$

These two objects encode both the system dynamic and the evolution of the configurational bath states. In fact,

$$\rho_S(t) = (1|\rho_t), \quad P_R(t) = (R|P_t), \quad (8)$$

where we have defined the R -vector $(1| \equiv \sum_R (R|$. These identities follows straightforwardly from Eqs. (1) and (2) respectively. The normalization of the system state can be written as $\text{Tr}_S[(1|\rho_t)] = 1$, while the normalization of the configurational populations read $(1|P_t) = 1$.

With the vectorial notation, the Lindblad rate equation (3) can be rewritten as

$$\frac{d|\rho_t\rangle}{dt} = \hat{\mathcal{L}}|\rho_t\rangle. \quad (9)$$

The structure of the matrix of system superoperators $\hat{\mathcal{L}}$ follows from (3). From now on, with the hat symbol we denote vectors in the R -space whose components are superoperators acting on the system Hilbert space.

III. QUANTUM-JUMP APPROACH

Our goal is to characterize the photon emission process associated to the fluorescent system. Of special interest is to determine how the environment fluctuations broke the renewal property in successive photon emissions. This property, for example, can be easily determine from a single experimental realization by measuring the successive time intervals, $\{\tau_i = t_i - t_{i-1}\}$, between consecutive photon recording events (happening at times t_i and t_{i-1}). Then, one can define the waiting time distribution

$$w_\infty^{(1)}(\tau) \equiv \langle \delta(\tau - \tau_i) \rangle_{\text{real}}, \quad (10)$$

where $\langle \dots \rangle_{\text{real}}$ denotes a time average along a single realization $[\langle f(\tau_i) \rangle_{\text{real}} = \lim_{t \rightarrow \infty} (1/t) \int_0^t dt' f(\tau_i(t'))]$. Consequently, $w_\infty^{(1)}(\tau_1)$ defines the *stationary* probability density of the intervals $\{\tau_i\}$. It satisfies the normalization $\int_0^\infty d\tau w_\infty^{(1)}(\tau) = 1$. Similarly, one can define the (stationary) probability distribution $w_\infty^{(2)}(\tau_2, \tau_1)$ for two consecutive intervals (τ_i and τ_{i+1}), i.e.,

$$w_\infty^{(2)}(\tau_2, \tau_1) \equiv \langle \delta(\tau_2 - \tau_{i+1}) \delta(\tau_1 - \tau_i) \rangle_{\text{real}}. \quad (11)$$

It fulfills $\int_0^\infty d\tau_2 \int_0^\infty d\tau_1 w_\infty^{(2)}(\tau_2, \tau_1) = 1$, and the consistency relations $\int_0^\infty d\tau_2 w_\infty^{(2)}(\tau_2, \tau_1) = w_\infty^{(1)}(\tau_1)$, and $\int_0^\infty d\tau_1 w_\infty^{(2)}(\tau_2, \tau_1) = w_\infty^{(1)}(\tau_2)$.

By knowing both probability distributions, one can quantify how much the photon emission process departs from a renewal one. The departure from zero of the dimensionless parameter

$$\Lambda(\tau_2, \tau_1) \equiv \frac{w_\infty^{(2)}(\tau_2, \tau_1)}{w_\infty^{(1)}(\tau_2) w_\infty^{(1)}(\tau_1)} - 1, \quad (12)$$

measures the strength of the non-renewal effects induced by the bath fluctuations. In fact, in absence of fluctuations the system dynamics becomes Markovian obeying the relation $w_\infty^{(2)}(\tau_2, \tau_1) = w_\infty^{(1)}(\tau_2) w_\infty^{(1)}(\tau_1)$, implying $\Lambda(\tau_2, \tau_1) = 0$. Nevertheless, we remark that non-Markovian system dynamic may also lead to renewal emission process [33–35].

The possibility of finding analytical expressions for $w_\infty^{(1)}(\tau_1)$ and $w_\infty^{(2)}(\tau_2, \tau_1)$ are one of the central results of this contribution. We solve this task by extending the quantum-jump approach on the basis of Eq. (9) [Eq. (3)].

A. Measurement operators

The quantum-jump approach relies on a quantum measurement theory [1–3]. Here, the definition of a measurement operation must to include both the system and the configurational bath states. If $|\rho\rangle$ is the state previous to a measurement, the state $\hat{\mathcal{M}}_\mu|\rho\rangle$ after measurement is

$$\hat{\mathcal{M}}_\mu|\rho\rangle = \frac{\hat{\mathcal{J}}_\mu|\rho\rangle}{\text{Tr}_S[(1|\hat{\mathcal{J}}_\mu|\rho)]}. \quad (13)$$

The vectorial superoperator $\hat{\mathcal{J}}_\mu$ define the unnormalized transformation of $|\rho\rangle$ due to the measurement action.

When not any measurement is performed over the configurational space, one must to consider only one superoperator $\hat{\mathcal{M}}_\mu$ associated to the photon detection events, $\mu \rightarrow \text{photon-detector}$ [see Eqs. (42) and (68)]. Nevertheless, we will also consider the existence of extra measurement channels that may provide information about the configurational states of the reservoir [see Eqs. (A2) and (A10)]. Hence, Eq. (9) is discomposed as

$$\frac{d|\rho_t\rangle}{dt} = (\hat{\mathcal{D}} + \sum_\mu \hat{\mathcal{J}}_\mu)|\rho_t\rangle, \quad (14)$$

where $\hat{\mathcal{D}} \equiv \hat{\mathcal{L}} - \sum_\mu \hat{\mathcal{J}}_\mu$. In the Markovian case, i.e., when the configurational space is one-dimensional, the (unique) superoperator $\hat{\mathcal{J}}_\mu$ is related to the wave vector collapse after a photon recording event, while $\hat{\mathcal{D}}$ defines the conditional dynamic between consecutive photon-detections [1–3]. Here, the formalism must also to take into account the fluctuations of the environment, i.e., the vectorial nature of $|\rho_t\rangle$ and the existence of different channels (labeled by μ) that may also provide information about the transitions between the bath states.

Equation (14) provides us the basis for characterizing the recording process. The following formulation is general, being independent of both the specific structure of Eq. (3) and the definition of the measurement channels $\{\hat{\mathcal{M}}_\mu\}$. Specific examples are worked out in Section IV and Appendix A.

B. Statistic of the detection events

The statistics of the successive recording events can be obtained after writing the system dynamics as an integral over all possible measurement paths. The evolution Eq. (14) can formally be integrated as

$$|\rho_t\rangle = e^{\hat{\mathcal{D}}t}|\rho_0\rangle + \sum_\mu \int_0^t e^{\hat{\mathcal{D}}(t-\tau)} \hat{\mathcal{J}}_\mu |\rho_\tau\rangle d\tau, \quad (15)$$

which can straightforwardly be rewritten in terms of the measurement operators $\{\hat{\mathcal{M}}_\mu\}$ as

$$\begin{aligned} |\rho_t\rangle &= P_0[t, 0; |\rho_0\rangle] \hat{\mathcal{T}}(t, 0) |\rho_0\rangle \\ &+ \sum_\mu \int_0^t P_0[t, \tau; \hat{\mathcal{M}}_\mu |\rho_\tau\rangle] \hat{\mathcal{T}}(t, \tau) \hat{\mathcal{M}}_\mu |\rho_\tau\rangle F_\mu[|\rho_\tau\rangle] d\tau. \end{aligned} \quad (16)$$

Here, we have introduced the non-unitary propagator

$$\hat{\mathcal{T}}(t, \tau) |\rho\rangle \equiv \frac{e^{\hat{\mathcal{D}}(t-\tau)} |\rho\rangle}{\text{Tr}_S[(1|e^{\hat{\mathcal{D}}(t-\tau)} |\rho\rangle)]}, \quad (17)$$

the function

$$P_0[t, \tau; |\rho\rangle] \equiv \text{Tr}_S[(1|e^{\hat{\mathcal{D}}(t-\tau)} |\rho\rangle)], \quad (18)$$

and the scalar contribution

$$F_\mu[|\rho\rangle] \equiv \text{Tr}_S[(1|\hat{\mathcal{J}}_\mu|\rho)]. \quad (19)$$

By associating the propagator $\hat{\mathcal{T}}(t, \tau)$ with the (vectorial) conditional system dynamic between consecutive recording events (photon-detections or/and configurational transitions), the first line of Eq. (16) can be interpreted as the contribution of all measurement realizations where not any detection event happens up to time t . Consistently, the weight $P_0[t, \tau; |\rho\rangle]$ must to interpreted as the corresponding (survival) probability for not having any transition in the interval (τ, t) , given that the last one happened at time τ , where system state is $|\rho\rangle$.

The second line (integral term) of Eq. (16) can be read as the contribution of all realizations where a measurement event happens at time τ [represented by the action of $\hat{\mathcal{M}}_\mu$ on $|\rho_\tau\rangle$] and not any detection happen up to time t , which justifies the presence of $\hat{\mathcal{T}}(t, \tau)$ and the survival probability $P_0[t, \tau; \hat{\mathcal{M}}_\mu |\rho_\tau\rangle]$. Consistently, $F_\mu[|\rho_\tau\rangle] d\tau$ must to define the probability of having an event in the μ -detector in the time interval $(\tau, \tau + d\tau)$.

By expressing Eq. (16) as a sum over all possible measurement outcomes, the previous statistical interpretation can explicitly be demonstrated. By writing

$$|\rho_t\rangle = \hat{\mathcal{G}}(t) |\rho_0\rangle = \sum_{n=0}^{\infty} \hat{\mathcal{G}}^{(n)}(t) |\rho_0\rangle, \quad (20)$$

with $\hat{\mathcal{G}}^{(0)}(t) = P_0[t, 0; |\rho_0\rangle] \hat{\mathcal{T}}(t, 0)$, from Eq. (16) we get

$$\begin{aligned} \hat{\mathcal{G}}^{(n)}(t) &= \sum_{\mu_n \dots \mu_1} \int_0^t dt_n \dots \int_0^{t_2} dt_1 P_n[t, \{t_i\}_1^n, \{\mu_i\}_1^n] \\ &\times \hat{\mathcal{T}}(t, t_n) \hat{\mathcal{M}}_{\mu_n} \dots \hat{\mathcal{T}}(t_2, t_1) \hat{\mathcal{M}}_{\mu_1} \hat{\mathcal{T}}(t_1, 0). \end{aligned} \quad (21)$$

The weight $P_n[t, \{t_i\}_1^n, \{\mu_i\}_1^n]$ is defined by

$$P_n[t, \{t_i\}_1^n, \{\mu_i\}_1^n] = P_0[t, t_n; \hat{\mathcal{M}}_{\mu_n} | \rho_{t_n}]) w_{\mu_n}[t_n, t_{n-1}; \hat{\mathcal{M}}_{\mu_{n-1}} | \rho_{t_{n-1}}]) \cdots w_{\mu_2}[t_2, t_1; \hat{\mathcal{M}}_{\mu_1} | \rho_{t_1}]) w_{\mu_1}[t_1, 0; | \rho_0]). \quad (22)$$

The intermediate states read

$$|\rho_{t_{i+1}}\rangle = \hat{\mathcal{T}}(t_{i+1}, t_i) \hat{\mathcal{M}}_{\mu_i} |\rho_{t_i}\rangle, \quad (23)$$

with $|\rho_{t_1}\rangle = \hat{\mathcal{T}}(t_1, 0) |\rho_0\rangle$, while

$$w_\mu[t, \tau; |\rho\rangle] \equiv \text{Tr}_S[(1 | \hat{\mathcal{J}}_\mu e^{\hat{\mathcal{D}}(t-\tau)} |\rho\rangle]. \quad (24)$$

Clearly, $\hat{\mathcal{G}}^{(n)}(t)$ [Eq. (21)] can be associated to all trajectories where n -detection events happen up to time t , each one at times $\{t_i\}_{i=1}^n$ in the $\{\mu_i\}_1^n$ detectors. The intermediate evolution between detection events $[\hat{\mathcal{M}}_{\mu_i}]$ is given by $\hat{\mathcal{T}}(t_i, t_{i-1})$. Consistently, $P_n[t, \{t_i\}_1^n, \{\mu_i\}_1^n]$ [Eq. (22)] defines the probability density of each trajectory. Thus, $w_{\mu_i}[t_i, t_{i-1}; \hat{\mathcal{M}}_{\mu_{i-1}} | \rho_{t_{i-1}}]) dt_i$ can be read as the probability of having a detection event in the μ_i -detector in the interval $(t_i, t_i + dt_i)$ given that the last detection event happened at time t_{i-1} in the μ_{i-1} -detector, not happening any event inside the interval (t_{i-1}, t_i) .

By using the normalization of the vectorial state, $(d/dt)\text{Tr}_S[(1 | \rho_t)] = 0$, from Eq. (14) it follows the relation $\text{Tr}_S[(1 | \hat{\mathcal{D}} | \bullet)] = -\sum_\mu \text{Tr}_S[(1 | \hat{\mathcal{J}}_\mu | \bullet)]$. Then, Eq. (18) can alternatively be written as

$$P_0[t, \tau; |\rho\rangle] = 1 - \sum_\mu \int_0^t w_\mu[t, \tau; |\rho\rangle] d\tau. \quad (25)$$

With this relation, we notice that Eq. (22) has the same structure than a renewal process, i.e., there exist a probability distribution (waiting time distribution, $w_\mu[t, \tau; |\rho\rangle]$) that define the statistic of the time interval between consecutive detection events. Nevertheless, here the waiting time distribution has a functional dependence on the system state posterior to a detection event $[\hat{\mathcal{M}}_\mu | \rho]$, which broke the renewal property.

By writing the states $|\rho_{t_{i+1}}\rangle$ [Eq. (23)] as

$$|\rho_{t_{i+1}}\rangle = \frac{e^{\hat{\mathcal{D}}(t_{i+1}-t_i)} \hat{\mathcal{J}}_{\mu_i} |\rho_{t_i}\rangle}{\text{Tr}_S[(1 | e^{\hat{\mathcal{D}}(t_{i+1}-t_i)} \hat{\mathcal{J}}_{\mu_i} | \rho_{t_i})]}, \quad (26)$$

the n -joint probability density (22) can be rewritten as

$$P_n[t, \{t_i\}_1^n, \{\mu_i\}_1^n] = \text{Tr}_S[(1 | e^{\hat{\mathcal{D}}(t-t_n)} \hat{\mathcal{J}}_{\mu_n} \cdots \hat{\mathcal{J}}_{\mu_2} e^{\hat{\mathcal{D}}(t_2-t_1)} \times \hat{\mathcal{J}}_{\mu_1} e^{\hat{\mathcal{D}}t_1} | \rho_0)]. \quad (27)$$

This expression recovers the result of Ref. [33]. Notice that its structure is similar to that obtained in the context of a photon measurement theory [1–3]. Nevertheless, here the underlying trajectories are vectorial and depend on the extra parameters μ_i , $i = 1 \cdots n$.

The probabilities $P_n(t)$ of having n -detection events up to time t can be obtained by integrating the joint

probabilities densities $P_n[t, \{t_i\}_1^n, \{\mu_i\}_1^n]$ over all possible detection paths

$$P_n(t) = \sum_{\mu_n \cdots \mu_1} \int_0^t dt_n \cdots \int_0^{t_2} dt_1 P_n[t, \{t_i\}_1^n, \{\mu_i\}_1^n]. \quad (28)$$

In the context of SMS, objects of this kind are usually characterized through a generating function approach based on a stochastic Bloch equation [26–30]. Then, while previous approaches are able to get these objects, the present treatment also allows us to get the underlying joint statistic defined by Eq. (22).

C. Stationary waiting time distributions

The joint probability density Eq. (22) is one of the central results of this section. It completely characterizes the statistic of the recording events. It can experimentally be determined from an ensemble average over measurement realizations having n -detection events in the interval $(0, t)$. Nevertheless, the stationary waiting time distributions Eqs. (10) and (11) are defined by a time average along a single measurement realization. For ergodic environment fluctuations, objects of this nature can be studied by describing the measurement process after happening an infinite number of recording events and that an infinite time elapsed since the initial condition, $|\rho_0\rangle$. In Appendix B, we show that in that limit Eq. (22) remains valid under the replacement

$$|\rho_0\rangle \rightarrow \hat{\mathcal{M}} |\rho_\infty\rangle, \quad (29)$$

where $|\rho_\infty\rangle$ corresponds to the stationary state

$$|\rho_\infty\rangle \equiv \lim_{t \rightarrow \infty} |\rho_t\rangle. \quad (30)$$

It comes forth because a time averaging procedure can only provide information about stationary observables. The measurement operator $\hat{\mathcal{M}}$ is defined by

$$\hat{\mathcal{M}} |\rho\rangle \equiv \frac{\hat{\mathcal{J}} |\rho\rangle}{\text{Tr}_S[(1 | \hat{\mathcal{J}} | \rho)]}, \quad \hat{\mathcal{J}} \equiv \sum_\mu \hat{\mathcal{J}}_\mu, \quad (31)$$

and takes into account the happening of an arbitrary measurement event in the long time regime. With these definitions, from Eq. (22) we introduce the first stationary waiting time distribution

$$w_\infty^{(1)}(\tau, \mu) \equiv w_\mu[\tau, 0; \hat{\mathcal{M}} | \rho_\infty] \quad (32)$$

$$= \text{Tr}_S[(1 | \hat{\mathcal{J}}_\mu e^{\hat{\mathcal{D}}\tau} \hat{\mathcal{M}} | \rho_\infty)],$$

as well as the second order stationary waiting time distribution

$$\begin{aligned} w_{\infty}^{(2)}(\tau_2, \mu_2; \tau_1, \mu_1) &\equiv w_{\mu_2}[\tau_2 + \tau_1, \tau_1; \hat{\mathcal{M}}_{\mu_1} | \rho_{\tau_1}] \\ &\quad \times w_{\mu_1}[\tau_1, 0; \hat{\mathcal{M}} | \rho_{\infty}] \\ &= \text{Tr}_S[(1 | \hat{\mathcal{J}}_{\mu_2} e^{\hat{\mathcal{D}}\tau_2} \hat{\mathcal{J}}_{\mu_1} e^{\hat{\mathcal{D}}\tau_1} \hat{\mathcal{M}} | \rho_{\infty})]. \end{aligned} \quad (33)$$

Higher objects, $w_{\infty}^{(n)}[\{\tau_i\}_1^n, \{\mu_i\}_1^n]$, can be written in a similar way. They define, in the stationary regime, the probability density of the time intervals $\{\tau_i\}_1^n$ between successive recording events happening in the $\{\mu_i\}_1^n$ detectors. When the measurement process only involves a photon detector apparatus, $\mu \rightarrow \text{photon-detector}$, Eqs.(32) and (33) allow to get analytical expressions for the distributions (10) and (11) respectively (see Section IV).

D. Stochastic density matrix evolution

From the previous analysis, we obtained the recording event statistics associated to the density matrix evolution Eq. (14). The quantum-jump approach also allows building up the underlying stochastic dynamics that reproduce that statistic. The key ingredient is the definition of a stochastic process developing in the system Hilbert space and whose realizations can be mapped with the realizations of the measurement apparatus signals. The average over realizations must to recover the system density matrix evolution. Then, in the present context we search for the definition of a stochastic vector $|\rho_t^{\text{st}}\rangle$, such that $\overline{|\rho_t^{\text{st}}\rangle} = |\rho_t\rangle$, where $|\rho_t\rangle$ is defined by the evolution (14). From now on, the overbar denotes (ensemble) averaging over realizations.

Based on the path integral solution obtained previously [Eq. (20)], the stochastic evolution can be written as a piecewise deterministic processes [3]

$$\frac{d}{dt} |\rho_t^{\text{st}}\rangle = [\hat{\mathcal{D}} - \text{Tr}_S(1 | \hat{\mathcal{D}} | \rho_t^{\text{st}})] |\rho_t^{\text{st}}\rangle + \sum_{\mu} (\hat{\mathcal{M}}_{\mu} - 1) |\rho_t^{\text{st}}\rangle \frac{dN_t^{\mu}}{dt}. \quad (34)$$

Here, the deterministic non-linear term [first contribution on the r.h.s.] corresponds to the *conditional* evolution in the intervals between consecutive measurements events, i.e., the dynamics defined by Eq. (17). On the other hand, the second term introduces the disruptive changes in the vectorial state after a measurement event, i.e., $|\rho_t^{\text{st}}\rangle \rightarrow \hat{\mathcal{M}}_{\mu} |\rho_t^{\text{st}}\rangle$. Consistently, the noisy terms are defined by $dN_t^{\mu}/dt \equiv \sum_k \delta(t - t_k^{\mu})$, where t_k^{μ} are the times where a measurement event happens in the μ -detector. By denoting with N_t^{μ} the number of detections events up to time t , it follows the alternative definition $dN_t^{\mu} = (N_{t+dt}^{\mu} - N_t^{\mu})$, i.e., dN_t^{μ} are the increments of the (Poisson) process N_t^{μ} [3]. In agreement with the previous analysis, their average must to recover Eq. (19), i.e.,

$$\overline{dN_t^{\mu}} = \text{Tr}_S[(1 | \hat{\mathcal{J}}_{\mu} | \rho_t)] dt = F_{\mu} [|\rho_t\rangle] dt. \quad (35)$$

By using the property $dN_t^{\mu} dN_t^{\mu'} = \delta_{\mu\mu'} dN_t^{\mu}$, which implies that a simultaneous detection in two different measurement apparatus is never observed and that $(dN_t^{\mu})^k = dN_t^{\mu}$, in Appendix C we show that Eq. (14) is recovered after averaging Eq. (34) over realizations.

The realizations associated to Eq. (34) can be easily determine after providing a recipe for calculating the random times where the detection events happen. Their numerical calculation relies on evaluating the statistical objects introduced in Eq. (16) along each trajectory. Given that the system is in the state $|\rho_t^{\text{st}}\rangle$, the quantity $F_{\mu} [|\rho_t^{\text{st}}\rangle] dt$ [Eq. (19)] gives the probability of having an event in the μ -detector in the time interval $(t, t + dt)$. This quantity defines an infinitesimal time step algorithm (see Appendix D). In a similar way, $P_0[t, t'; \hat{\mathcal{M}}_{\mu} | \rho_{t'}^{\text{st}}]$ [Eq. (18)] define the survival probability for the next detection event (at time t) given that a μ -detection event happened at time t' . This object allows to defining a finite time step algorithm (see Appendix D).

Independently of the method (algorithm) used to determine the times of the recording events (transitions), given that at time t a measurement happens, $|\rho_t^{\text{st}}\rangle \rightarrow \hat{\mathcal{M}}_{\mu} |\rho_t^{\text{st}}\rangle$, each transformation $\hat{\mathcal{M}}_{\mu}$ [Eq. (13)] must be chosen with probability

$$t_{\mu}(t) \equiv \frac{F_{\mu} [|\rho_t^{\text{st}}\rangle]}{\sum_{\mu'} F_{\mu'} [|\rho_t^{\text{st}}\rangle]} = \frac{\text{Tr}_S[(1 | \hat{\mathcal{J}}_{\mu} | \rho_t^{\text{st}})]}{\sum_{\mu'} \text{Tr}_S[(1 | \hat{\mathcal{J}}_{\mu'} | \rho_t^{\text{st}})]}, \quad (36)$$

which satisfy $\sum_{\mu} t_{\mu}(t) = 1$. This rule corresponds to a selective measurement of the set of μ -observables [3]. Between successive recording events, the evolution of $|\rho_t^{\text{st}}\rangle$ is deterministic and defined by Eq. (17).

Through the relations

$$\rho_S^{\text{st}}(t) \equiv (1 | \rho_t^{\text{st}}), \quad |P_t^{\text{st}}\rangle \equiv \text{Tr}_S[|\rho_t^{\text{st}}\rangle], \quad (37)$$

the vectorial state $|\rho_t^{\text{st}}\rangle$ provide a stochastic representation of both the system density matrix [Eq. (1)], $\overline{\rho_S^{\text{st}}(t)} = \rho_S(t)$, and the occupation of the configurational bath states [Eq. (2)], $\overline{(R | P_t^{\text{st}})} = P_R(t)$. In contrast with the standard quantum-jump approach, in general it is not possible to get a simple dynamical evolution for $\rho_S^{\text{st}}(t)$ [or to $(R | P_t^{\text{st}})$]. In fact, here the formalism relies on the vectorial nature of $|\rho_t^{\text{st}}\rangle$ [however see also Appendix A].

E. Non-renewal recording realizations

The trajectories associated to Eq. (34) allow us to establishing a simple scheme for understanding the *non-renewal* nature of the recording process. In fact, its underlying structure is similar to that of a renewal one. Given that the last event happened at time t' in the μ -detector, the random time t for the next event is defined by a waiting time distribution $w_{\text{st}}(t, t', \mu)$, which read

$$w_{\text{st}}(t, t', \mu) \equiv -\frac{d}{dt} P_0[t, t'; \hat{\mathcal{M}}_{\mu} | \rho_{t'}^{\text{st}}], \quad (38a)$$

$$= -\text{Tr}_S[(1 | \hat{\mathcal{D}} e^{\hat{\mathcal{D}}(t-t')} \hat{\mathcal{M}}_{\mu} | \rho_{t'}^{\text{st}})]. \quad (38b)$$

By using the relation $\text{Tr}_S[(1|\hat{\mathcal{D}}|\bullet)] = -\sum_\mu \text{Tr}_S[(1|\hat{\mathcal{J}}_\mu|\bullet)]$, it follows

$$w_{\text{st}}(t, t', \mu) = \text{Tr}_S[(1|\hat{\mathcal{J}} e^{\hat{\mathcal{D}}(t-t')} \hat{\mathcal{M}}_\mu |\rho_{t'}^{\text{st}})], \quad (39)$$

where $\hat{\mathcal{J}} = \sum_\mu \hat{\mathcal{J}}_\mu$ [Eq. (31)]. At time t , $|\rho_t^{\text{st}}\rangle$ is updated with the conditional evolution Eq. (17) and the new recording event is selected with the probabilities (36). The next events follow from the same rule (see Appendix D). The average over realizations recover the statistics defined by Eq. (22).

The departure of the recording realizations with respect to a renewal process comes from the dependence of $w_{\text{st}}(t, t', \mu)$ on $|\rho_{t'}^{\text{st}}\rangle$. Only if $\hat{\mathcal{M}}_\mu |\rho_{t'}^{\text{st}}\rangle$ is independent of $|\rho_{t'}^{\text{st}}\rangle$ one get a renewal recording process. Nevertheless, in general this does not happen, implying that $w_{\text{st}}(t, t', \mu)$ randomly change between successive events. Then, in contrast with a renewal process, here the successive events are defined by a stochastic waiting time distribution that parametrically depends on the vectorial state $|\rho_{t'}^{\text{st}}\rangle$. Finally, we notice that $w_{\text{st}}(t, t', \mu)$ can consistently be written as $w_{\text{st}}(t, t', \mu) = \sum_{\tilde{\mu}} w_{\tilde{\mu}}[t, t'; \hat{\mathcal{M}}_\mu |\rho_{t'}^{\text{st}}\rangle]$, where $w_\mu[t, t'; \rho]$ is defined by Eq. (24).

IV. PHOTON EMISSION MEASUREMENTS

In the previous sections, we developed a general theory that allows to characterizing the measurement processes associated to a broad class of physical situation arising in SMS. The theory depends on which kind of measurement process is performed over both the system and the configurational states. In this section, we analyze the situation where there exists only one measurement process defined by a photon detector apparatus coupled to the scattered electromagnetic field. This is the standard situation in SMS, where any direct information about the configurational space is unavailable. Then, the parameter μ only includes one term corresponding to the photon detector. Furthermore, our formalism is able to describe different kind of environmental fluctuations. First, we analyze the case of self-fluctuating environments, i.e., when the transitions between the configurational states do not depend on the state of the system. As a second leading case, we analyze environmental fluctuations that depend on the intensity of the laser excitation.

A. Self-fluctuating environments

This case is covered by Eq. (3) by taking $A = I$,

$$\begin{aligned} \frac{d\rho_R(t)}{dt} = & \frac{-i}{\hbar} [H_R, \rho_R(t)] - \gamma_R \{ \{D, \rho_R(t)\}_+ - \mathcal{J}[\rho_R(t)] \} \\ & - \sum_{R'} \phi_{R'R} \rho_R(t) + \sum_{R'} \phi_{RR'} \rho_{R'}(t). \end{aligned} \quad (40)$$

For notational consistency we take $\eta_{RR'} \rightarrow \phi_{RR'}$ [31]. From Eq. (40), the evolution of populations Eq. (2) is

given by

$$\frac{d}{dt} P_R(t) = - \sum_{R'} \phi_{R'R} P_R(t) + \sum_{R'} \phi_{RR'} P_{R'}(t). \quad (41)$$

Hence, the stochastic dynamics between the configurational states is governed by a classical master equation that does not depend on the state of the system. This case allow to describe processes such as spectral fluctuations, life time fluctuations, and molecules diffusing in a solution.

1. Photon measurement operator

The measurement operator, Eq. (13), must to take into account all contributions that, independently of the R -state of the reservoir, lead to a photon emission. Then, from Eq. (40), we write ($\mu \rightarrow \text{ph}$) $[|\rho\rangle = \sum_R |R\rangle \rho_R]$

$$\hat{\mathcal{M}}_{\text{ph}} |\rho\rangle = \frac{\hat{\mathcal{J}}_{\text{ph}} |\rho\rangle}{\text{Tr}_S[(1|\hat{\mathcal{J}}_{\text{ph}}|\rho)]} = \frac{\sum_R \gamma_R |R\rangle \sigma \rho_R \sigma^\dagger}{\sum_{R'} \gamma_{R'} \text{Tr}_S[\sigma^\dagger \sigma \rho_{R'}]}. \quad (42)$$

Notice that each contribution in the sum corresponds to the standard definition arising in Markovian fluorescent systems [1–3], i.e., $\hat{\mathcal{M}}_{\text{ph}} \rho = \sigma \rho \sigma^\dagger / \text{Tr}_S[\sigma^\dagger \sigma \rho]$. The vectorial superoperator $\hat{\mathcal{D}}$ [Eq. (14)] here is defined from

$$\hat{\mathcal{D}} = \hat{\mathcal{L}} - \hat{\mathcal{J}}_{\text{ph}}, \quad (43)$$

where $\hat{\mathcal{L}}$ follows from Eqs. (9) and (40), while $\hat{\mathcal{J}}_{\text{ph}}$ from Eq. (42). Alternatively, $\hat{\mathcal{D}}$ can be explicitly defined through the non-unitary evolution generated by it

$$\frac{d}{dt} (R|\rho_t^{\text{u}}) = (R|\hat{\mathcal{D}}|\rho_t^{\text{u}}), \quad (44)$$

where the index u say us that the auxiliary vector $|\rho_t^{\text{u}}\rangle$ is not normalized to one. In fact, its norm is related to the survival probability Eq. (18). By denoting $\rho_R^{\text{u}}(t) = (R|\rho_t^{\text{u}})$, we get

$$\begin{aligned} \frac{d\rho_R^{\text{u}}(t)}{dt} = & \frac{-i}{\hbar} [H_R, \rho_R^{\text{u}}(t)] - \gamma_R \{ D, \rho_R^{\text{u}}(t) \}_+ \\ & - \sum_{R'} \phi_{R'R} \rho_R^{\text{u}}(t) + \sum_{R'} \phi_{RR'} \rho_{R'}^{\text{u}}(t). \end{aligned} \quad (45)$$

Having the definition of the superoperators $\hat{\mathcal{M}}_{\text{ph}}$ and $\hat{\mathcal{D}}$ we can apply the theory developed in previous section.

2. Stochastic dynamics

The dynamic of the stochastic state $|\rho_t^{\text{st}}\rangle$ follows from Eq. (34). The disruptive transformation associated to a photon detection event, $|\rho_t^{\text{st}}\rangle \rightarrow \hat{\mathcal{M}}_{\text{ph}} |\rho_t^{\text{st}}\rangle$, from the expression (42), and by using that $\sigma = |-\rangle \langle +|$, $\sigma^\dagger = |+\rangle \langle -|$, can explicitly be written as

$$|\rho_t^{\text{st}}\rangle \rightarrow \hat{\mathcal{M}}_{\text{ph}} |\rho_t^{\text{st}}\rangle = |-\rangle \langle -| \sum_R p_R^{\text{st}}(t) |R\rangle. \quad (46)$$

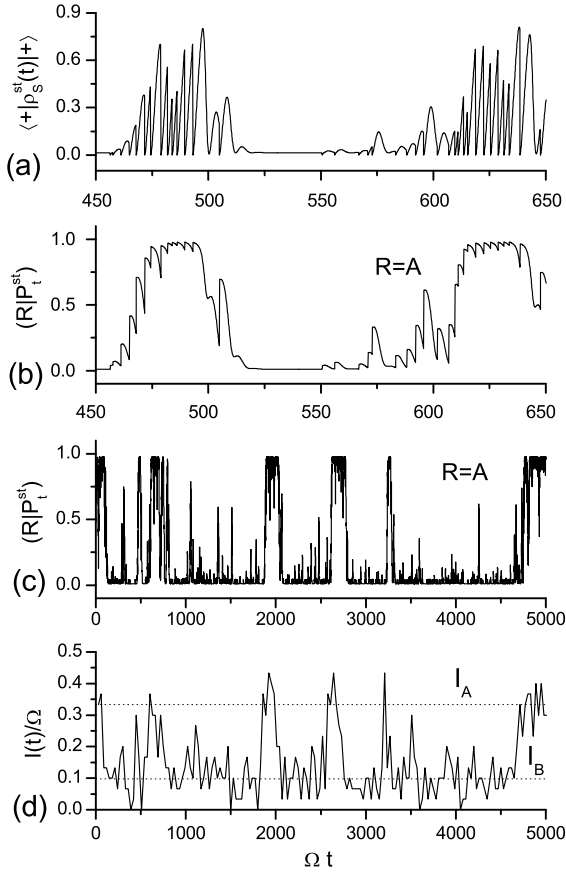


FIG. 1: Stochastic realizations of a fluorophore system defined by the evolution Eq. (40). The configurational space is two-dimensional, $R = A, B$. The parameters are $\Omega_R = \Omega$, $\delta\omega_R = 0$, $\gamma_A/\Omega = 1$, $\gamma_B/\Omega = 10$, $\phi_{AB}/\Omega = 0.003$, $\phi_{BA}/\Omega = 0.009$. The laser is in resonance with the system, i.e., $\omega_L = \omega_0$. (a) Realization of the upper population of the system $\langle + | \rho_S^{\text{st}}(t) | + \rangle$. (b)-(c) Realization of the configurational population of the bath $(R|P_t^{\text{st}})$, for $R = A$. (d) Intensity realization. The values I_R are defined by Eq. (50).

Here, the weights $\{p_R^{\text{st}}(t)\}$ satisfy the normalization $\sum_R p_R^{\text{st}}(t) = 1$, and are defined as

$$p_R^{\text{st}}(t) \equiv \frac{\gamma_R \langle + | \rho_R^{\text{st}}(t) | + \rangle}{\sum_{R'} \gamma_{R'} \langle + | \rho_{R'}^{\text{st}}(t) | + \rangle}, \quad (47)$$

where the notation $\rho_R^{\text{st}}(t) = (R|\rho_t^{\text{st}})$ was used. From Eqs. (37) and (46), it is simple to get

$$\rho_S^{\text{st}}(t) \rightarrow (1|\hat{\mathcal{M}}_{\text{ph}}|\rho_t^{\text{st}}) = |-\rangle \langle -|, \quad (48)$$

and that

$$(R|P_t^{\text{st}}) \rightarrow \text{Tr}_S[(R|\hat{\mathcal{M}}_{\text{ph}}|\rho_t^{\text{st}})] = p_R^{\text{st}}(t). \quad (49)$$

Eq. (48) shows that in fact, after a photon detection event the system collapses to its lower state $|-\rangle$. On the other hand, Eq. (49) says us that $p_R^{\text{st}}(t)$ is the value of the configurational populations after a photon recording event.

Between the detection events the stochastic dynamics is defined the conditional evolution defined by the super-operator $\hat{\mathcal{D}}$ [Eqs. (43) and (45)]. On the other hand, as there exist only one measurement apparatus, the weights $\{t_\mu(t)\}$, Eq. (36), here reduce to $t_{\text{ph}}(t) = 1$.

In the next figures, we consider a fluorophore system coupled to an environment characterized by a two-dimensional configurational space, $R = A, B$, which only affect the decay rates $\{\gamma_R\}$ of the system, i.e., the Rabi frequencies [Eq. (4)] do not depend on the configurational states, $\Omega_R = \Omega$, and the spectral shifts [Eq. (5)] are null, $\delta\omega_R = 0$. Furthermore, the laser is in resonance with the system, i.e., $\omega_L = \omega_0$.

In Fig. 1(a) we show a realization of the upper population of the system $\langle + | \rho_S^{\text{st}}(t) | + \rangle$ [Eq. (37)]. The realizations were determined by using the finite time step algorithm defined in Appendix D. Each collapse of the upper population to zero is related to a photon emission [see Eq. (48)].

In Fig. 1(b), we show the realization of the configurational population $(R|P_t^{\text{st}})$ for $R = A$ [Eq. (37)]. As the configurational space is two-dimensional, $(A|P_t^{\text{st}}) + (B|P_t^{\text{st}}) = 1$. We remark that these realizations are associated to a measurement process that only gives information about the photon emission events. Not any information is provided about the configurational states of the bath. Therefore, the realizations of $(R|P_t^{\text{st}})$ are the best estimation [40] about the configurational state of the reservoir that can be obtained by knowing the master equation (40) and a given realization of the photon detector apparatus.

In Fig 1(c) we plot $(R|P_t^{\text{st}})$ (for $R = A$) over a larger time interval. For the chosen parameter values, the configurational populations develop a quasi-dichotomic behavior. When $(R|P_t^{\text{st}}) \approx 1$, we can affirm that is highly probable that the bath is in the configurational state $|R\rangle$.

In Fig. 1(d), we plot the scattered intensity, which is defined by $I(t) = [n(t + \delta t) - n(t)]/\delta t$, where $n(t)$ is the number of photon recording events up to time t and δt is an adequate time flag averaging. Its fluctuations are highly correlated with the values of $(R|P_t^{\text{st}})$. In fact, the intensity fluctuates around two well-defined values I_R , which are defined by the intensity of a Markovian fluorescent system [1–3] characterized by the parameters corresponding to each configurational state [31], i.e.,

$$I_R = \frac{\gamma_R \Omega_R^2}{\gamma_R^2 + 2\Omega_R^2 + 4\delta_R^2}, \quad (50)$$

where $\delta_R \equiv \omega_L - \omega_R$. The dichotomic behavior arises because the system is able to emit a large number of photons previously to the occurrence of a transition between the configurational bath states, i.e., $\sum_{R'} \phi_{R'R} \ll I_R$.

In Fig. 2(a) we plot the upper population $\langle + | \rho_S(t) | + \rangle$ that follows from Eq. (40), as well as an average over ($\approx 10^3$) realizations of $\langle + | \rho_S^{\text{st}}(t) | + \rangle$ [see Fig. 1(a)]. In Fig. 2(b), we plot the analytical solution of the configurational populations $(R|P_t)$ defined by Eq. (41), as well as an average over realization of $(R|P_t^{\text{st}})$ [see Fig. 1(b) and

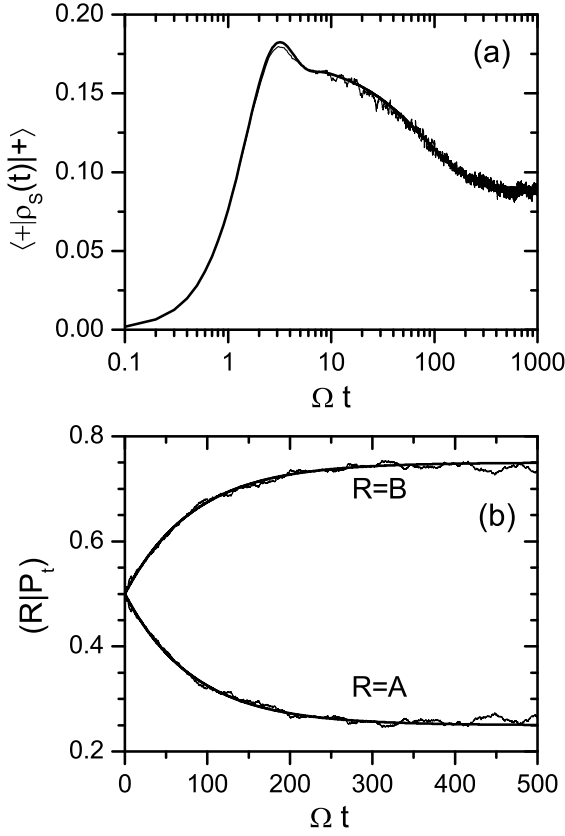


FIG. 2: Evolution of the upper population $\langle +|\rho_S(t)|+ \rangle$ (a) and the configurational populations $\langle R|P_t \rangle$ (b), that follows from Eqs. (40) and (41) respectively. The parameters are the same than in Figure 1. The initial conditions are $\rho_S(0) = |-\rangle \langle -|$ and $\langle A|P_0 \rangle = \langle B|P_0 \rangle = 1/2$. The noisy curves follow from an average over the realizations shown in Fig. 1.

(c)]. In both cases the ensemble averages recover the dynamics dictated by the corresponding master equations, showing the consistency of the developed approach.

3. Photon emission process

The recording events are characterized by the stochastic waiting time distribution Eq. (39). Then, we write

$$w_{st}(t, t') = \text{Tr}_S[(1|\hat{\mathcal{J}}e^{\hat{\mathcal{D}}(t-t')}\hat{\mathcal{M}}_{ph}|\rho_{t'}^{st})]. \quad (51)$$

Notice that here $\hat{\mathcal{J}} = \hat{\mathcal{J}}_{ph}$. The function $w_{st}(t, t')$ define the statistic of the time intervals between consecutive photon emissions. From Eqs. (42) and (46) it follows

$$w_{st}(t, t') = \sum_{RR'} \gamma_R \langle +|e_{RR'}^{\hat{\mathcal{D}}(t-t')}[|-\rangle \langle -|p_{R'}^{st}(t')]|+ \rangle. \quad (52)$$

This expression allows us to get an analytical expression for $w_{st}(t, t')$ [not provided due to its extension] that parametrically depends on the set $\{p_{R'}^{st}(t')\}$, Eq. (47).

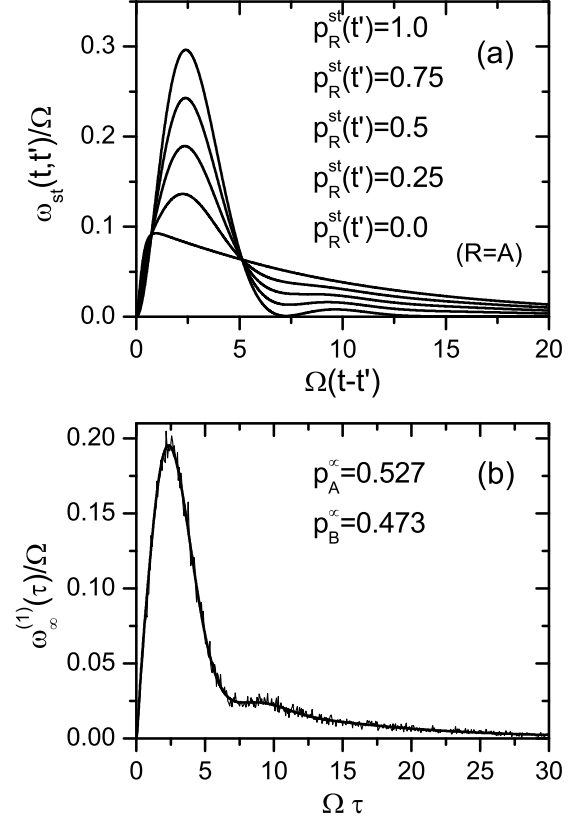


FIG. 3: (a) Plot of the waiting time distribution $w_{st}(t, t')$ [Eq. (52)] for different values of $p_R^{st}(t')$. From top to bottom we take $(R = A)$ $p_R^{st}(t') = 1, 0.75, 0.5, 0.25$ and 0 . (b) Stationary waiting time distribution [Eq. (53)]. The stationary weights [Eq. (55)] read $p_A^{\infty} = 0.527$ and $p_B^{\infty} = 0.473$. The noisy curve corresponds to a numerical distribution determine from the intervals between consecutive photon emissions [Eq. (10)] along a single realization (like that shown in Fig. 1). In both plots, the parameters are the same than in Fig. 1.

As the set of weights $\{p_{R'}^{st}(t')\}$ correspond to the configurational populations after a photon recording event [see Eq. (49)], the waiting time distribution change between consecutive photon emissions. The successive (stochastic) values of $\{p_{R'}^{st}(t')\}$ can be read from the realization of $\langle R|P_t^{st} \rangle$ shown in Fig. 1(b). Notice that in each event, defined by the collapses $\langle +|\rho_S^{st}(t)|+ \rangle \rightarrow 0$ [Fig. 1(a)], $\langle R|P_t^{st} \rangle$ suffer an abrupt change in its slope.

In Fig. 3(a), we plot $w_{st}(t, t')$ (as a function of $t - t'$) for different values of the parameters $p_{R'}^{st}(t')$. As the configurational space is two-dimensional, the two parameters satisfy the normalization $p_A^{st}(t') + p_B^{st}(t') = 1$. We notice that $w_{st}(t, t')$ has a strong dependence on the values of the configurational populations $\{p_{R'}^{st}(t')\}$, which in turn say us that the photon emission process strongly departs from a renewal one. For Markovian fluorescent systems, the set $\{p_{R'}^{st}(t')\}$ reduce to only one parameter with value equal to one (the configurational space is one-dimensional). Therefore, $w_{st}(t, t')$ is the same object along a measurement trajectory, recovering a renewal

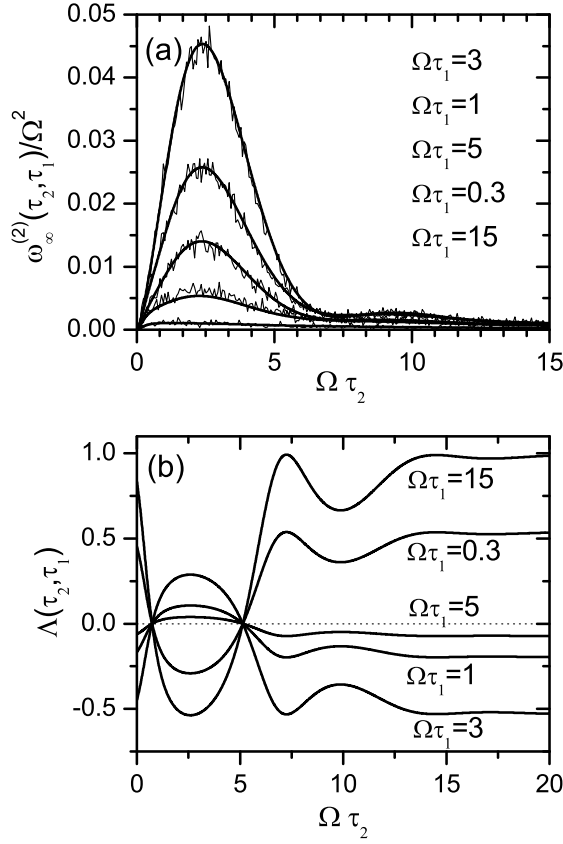


FIG. 4: (a) Stationary two-time waiting time distribution $w_\infty^{(2)}(\tau_2, \tau_1)$ [Eq. (56)] for different values of τ_1 . From top to bottom we take $\Omega\tau_1 = 3, 1, 5, 0.3$, and 15 . The noisy curves correspond to the time average Eq. (11). (b) Parameter $\Lambda(\tau_2, \tau_1)$ [Eq. (12)] determine from Eqs. (53) and (56), for different values of τ_1 . From top to bottom $\Omega\tau_1 = 15, 0.3, 5, 1$, and 3 . The parameters are the same than in Fig. 1.

process.

4. Stationary waiting time distributions

By measuring the time intervals between successive photon emissions along a given trajectory one can determine the stationary waiting time distribution Eq. (10). The analytical expression for this probability distribution can be read from Eq. (32). We get

$$w_\infty^{(1)}(\tau) = \sum_{RR'} \gamma_R \langle + | e^{\hat{D}_{RR'}\tau} | - \rangle \langle - | p_{R'}^\infty | + \rangle, \quad (53)$$

where the weights p_R^∞ are defined from the relation

$$\hat{\mathcal{M}}_{\text{ph}} |\rho_\infty\rangle = |-\rangle \langle - | \sum_R p_R^\infty | R \rangle, \quad (54)$$

delivering the expression

$$p_R^\infty \equiv \frac{\gamma_R \langle + | \rho_R^\infty | + \rangle}{\sum_{R'} \gamma_{R'} \langle + | \rho_{R'}^\infty | + \rangle}. \quad (55)$$

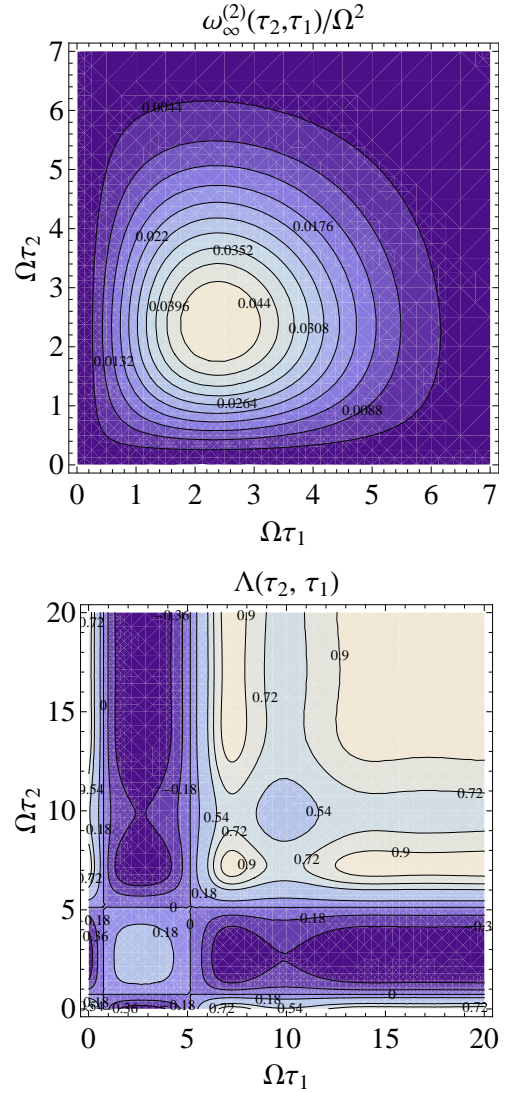


FIG. 5: Contour plot of $w_\infty^{(2)}(\tau_2, \tau_1)/\Omega^2$ [upper panel] and $\Lambda(\tau_2, \tau_1)$ [lower panel] corresponding to the plots of Fig. 4.

Here, $\rho_R^\infty \equiv \lim_{t \rightarrow \infty} \rho_R(t) = (R | \rho_\infty)$ [Eq. (30)]. By comparing Eq. (53) with Eq. (52), we realize that $w_\infty^{(1)}(\tau)$ follows from $w_{\text{st}}(t, t')$ after the replacements $p_{R'}^{\text{st}}(t') \rightarrow p_{R'}^\infty$ and $(t - t') \rightarrow \tau$.

In Fig. 3(b) we plot the analytical expression for $w_\infty^{(1)}(\tau)$ that follows from Eq. (53). Furthermore, we show a numerical distribution determine from the time average Eq. (10). The theoretical distribution correctly fit the numerical result. Consistently, we also checked that the time average of $\{p_R^{\text{st}}(t')\}$ along a single trajectory recover the weights $\{p_R^\infty\}$, Eq. (55).

The analytical expression for the second waiting time Eq. (11) can be obtained from Eq. (33), delivering

$$w_\infty^{(2)}(\tau_2, \tau_1) = \sum_{RR'} \gamma_R \langle + | e^{\hat{D}_{RR'}\tau_2} | - \rangle \langle - | \varphi_{R'}(\tau_1) | + \rangle, \quad (56)$$

where the functions $\varphi_R(\tau_1)$ read

$$\varphi_R(\tau_1) \equiv \gamma_R \sum_{R'} \langle + | e^{\hat{D}_{RR'}\tau_1} | - \rangle \langle - | p_{R'}^\infty | + \rangle. \quad (57)$$

In Fig. 4(a) we plot the analytical expression for $w_\infty^{(2)}(\tau_2, \tau_1)$ that follows from Eq. (56) for different values of τ_1 . Furthermore, we show the numerical result that follows by determining the probability distribution of two consecutive time intervals between successive photon emissions along a single trajectory, Eq. (11). The theoretical result correctly fit the numerical distribution.

In Fig. 4(b) we plot the dimensionless parameter $\Lambda(\tau_2, \tau_1)$ [Eq. (12)] determine from Eqs. (53) and (56), for different values of τ_1 . For almost all values of τ_2 and τ_1 , $\Lambda(\tau_2, \tau_1)$ departs appreciably from zero, indicating the departure of the photon emission process from a renewal one. We also note that there exist special values of the consecutive time intervals where $\Lambda(\tau_2, \tau_1) = 0$. From the definition Eq. (12), we deduce that when $\Lambda(\tau_2, \tau_1) > 0$, the frequency of the successive intervals τ_1 and τ_2 is greater than in the renewal case. The situation $\Lambda(\tau_2, \tau_1) < 0$, admits the inverse interpretation. For clarifying the structure of both $w_\infty^{(2)}(\tau_2, \tau_1)$ and $\Lambda(\tau_2, \tau_1)$, in Fig. 5 we show their contour plots. As can be deduced from Fig. 4 and 5, $\Lambda(\tau_2, \tau_1)$ reach it maximal values for higher values of both τ_2 and τ_1 .

5. Slow and fast environment fluctuations

The expressions for the stochastic waiting distribution $w_{\text{st}}(t, t')$ [Eq. (52)], and the first $[w_\infty^{(1)}(\tau), \text{Eq. (53)}]$ and second $[w_\infty^{(2)}(\tau_2, \tau_1), \text{Eq. (56)}]$ stationary waiting time distributions allow to characterize the photon emission process as well as its departure with respect to a renewal one. Here, we provide simple analytical expressions for these objects in the limit of both fast and slow environment fluctuations.

The characteristic time of the bath fluctuations are measured by the rates $\{\phi_{R'R}\}$, Eqs. (40) and (41). On the other hand, the average time between photon emissions is measured by the inverse of the intensities $\{I_R\}$, Eq. (50).

When the bath fluctuations are much slower than the average time between photon emissions, $\{\phi_{R'R}\} \ll \{I_R\}$, it is valid to approximate the conditional evolution defined by the superoperator \hat{D} [Eqs. (43) and (44)] as

$$e^{\hat{D}(t-t')} | - \rangle \langle - | p_{R'}^{\text{st}}(t') \rangle \approx \delta_{RR'} e^{\hat{D}_{RR}(t-t')} | - \rangle \langle - | p_R^{\text{st}}(t') \rangle. \quad (58)$$

This approximation corresponds to disregarding the non-diagonal contributions between photon recording events. By inserting this condition in Eq. (52) we get

$$\begin{aligned} w_{\text{st}}(t, t') &\simeq \sum_R \gamma_R \langle + | e^{\hat{D}_{RR}(t-t')} | - \rangle \langle - | p_R^{\text{st}}(t') | + \rangle, \\ &= \sum_R w_R(t-t') p_R^{\text{st}}(t'). \end{aligned} \quad (59)$$

Then, $w_{\text{st}}(t, t')$ can be written as a linear combination of the waiting time distributions $\{w_R(t)\}$, each one being defined by the expression

$$w_R(t) \equiv \gamma_R \langle + | e^{\hat{D}_{RR}t} | - \rangle \langle - | | + \rangle. \quad (60)$$

This function correspond to the waiting time distribution associated to a Markovian fluorescent system [1, 5] with decay rate γ_R , and whose Hamiltonian is given by H_R , Eq. (4), i.e., its transition frequency is $\omega_R = (\omega_0 + \delta\omega_R)$, and its coupling to the external laser is measured by Ω_R . This result can straightforwardly be read from Eqs. (44) and (45) under the replacement $\phi_{RR'} \rightarrow 0$. In the Laplace domain, $t \rightarrow u$, it can be written as [34]

$$w_R(u) = \frac{\gamma_R/2}{u + \gamma_R/2} \left(\frac{\Omega_R^2 h_R(u)}{u^2 + u\gamma_R + \Omega_R^2 h_R(u)} \right), \quad (61)$$

where the auxiliary function $h_R(u)$ is

$$h_R(u) = \frac{(u + \gamma_R/2)^2}{(u + \gamma_R/2)^2 + \delta_R^2}, \quad (62)$$

and $\delta_R = \omega_L - \omega_R$. After Laplace inversion, we get

$$w_R(t) = \frac{2\gamma_R\Omega_R^2}{\zeta_R} \exp(-\gamma_R t/2) [\cosh(\xi_R^+ t) - \cosh(\xi_R^- t)], \quad (63)$$

where $\xi_R^\pm = [\gamma_R^2 - 4(\Omega_R^2 + \delta_R^2) \pm \zeta_R]^{1/2}/(2\sqrt{2})$, with $\zeta_R = \{[\gamma_R^2 + 4(\Omega_R^2 + \delta_R^2)]^2 - 16\gamma_R^2\Omega_R^2\}^{1/2}$. When $\delta_R = 0$, the expression of Refs. [1, 5] is recovered.

We have checked that Eq. (59) joint with Eq. (63) provide an excellent approximation to the exact functions plotted in Fig. 3(a). On the other hand, Eq. (58) is also useful for approximating the stationary waiting time distributions. Eq. (53) leads to

$$w_\infty^{(1)}(\tau) \simeq \sum_R w_R(\tau) p_R^\infty, \quad (64)$$

while from Eq. (56), we get

$$w_\infty^{(2)}(\tau_2, \tau_1) \simeq \sum_R w_R(\tau_2) w_R(\tau_1) p_R^\infty. \quad (65)$$

Furthermore, under the hypothesis of slow fluctuations, from Eq. (40) we can approximate $\gamma_R \langle + | \rho_R^\infty | + \rangle \simeq I_R P_R^\infty$. The constants I_R [Eq. (50)] are the intensities associated to each configurational state R . On the other hand, P_R^∞ are the stationary values of the configurational populations Eq. (41), i.e., $P_R^\infty \equiv \lim_{t \rightarrow \infty} P_R(t)$. Therefore, from Eq. (55) we get the approximate expression

$$p_R^\infty \simeq \frac{I_R P_R^\infty}{\sum_{R'} I_{R'} P_{R'}^\infty}. \quad (66)$$

Eqs. (64), (65), and (66), also provide an excellent approximation to the exact analytical results plotted in Figs. 3, 4 and 5. Moreover, they have a clear physical meaning. In the slow limit each bath state establishes an

intensity regime defined by Eq. (50). Hence, the statistic of the non-renewal photon emission process follows from an average of the renewal statistic associated to each state [defined by $w_R(\tau)$]. The weight of each contribution is p_R^∞ . Consistently, this factors, which are the average configurational populations after a detection event [Eq. (54)], are proportional to the intensities I_R and the stationary populations P_R^∞ related to each bath state.

When the bath fluctuations are much faster than the average time between photon emissions, $\{\phi_{R'R}\} \gg \{I_R\}$, the configurational populations reach their stationary values, $P_R^\infty = \lim_{t \rightarrow \infty} P_R(t)$, before happening many photon emissions. Hence, the fluorophore behaves as a Markovian fluorescent system with decay rate $\bar{\gamma} \equiv \sum_R \gamma_R P_R^\infty$, Rabi frequency $\bar{\Omega} \equiv \sum_R \Omega_R P_R^\infty$, and detuning $\bar{\delta} \equiv \sum_R \delta_R P_R^\infty$. The photon emission process becomes a renewal one, being defined by the waiting time distribution Eq. (63) with $\{\gamma_R, \Omega_R, \delta_R\} \rightarrow \{\bar{\gamma}, \bar{\Omega}, \bar{\delta}\}$. Near of this limit, for two-dimensional configurational spaces, $w_\infty^{(2)}(\tau_2, \tau_1)$ develops small asymmetries on its arguments $w_\infty^{(2)}(\tau_2, \tau_1) \neq w_\infty^{(2)}(\tau_1, \tau_2)$. In general, this property may arise in the intermediate regime between fast, $w_\infty^{(2)}(\tau_2, \tau_1) \simeq w_\infty^{(1)}(\tau_2)w_\infty^{(1)}(\tau_1)$, and slow bath fluctuations, Eq. (65).

The configurational fluctuations are frozen when Eq. (40) is defined with $\{\phi_{R'R}\} = 0$. This case was partially addressed in Refs. [34, 35]. Our present treatment provides a general description. Evidently, the configurational populations remain unaffected during all the evolution, $|P_t\rangle = |P_0\rangle$. The results of Ref. [34, 35] follows from the approximation $|P_t^{\text{st}}\rangle \approx |P_0\rangle$, which is valid in a weak laser intensity regime and when the dynamics develops two different times scales induced by an infinite dimensional configurational space.

B. Light Assisted environment fluctuations

The general evolution Eq. (3) may also cover the case in which the statistical properties of the radiation pattern, as well as the environment fluctuations, depend on the external laser intensity [31, 36], i.e., light assisted processes. By taking $A = \sigma$, and $\eta_{RR'} \rightarrow \gamma_{RR'}$, we write

$$\frac{d\rho_R(t)}{dt} = \frac{-i}{\hbar} [H_R, \rho_R(t)] - \gamma_R \{D, \rho_R(t)\}_+ - \mathcal{J}[\rho_R(t)] - \sum_{R'} \gamma_{RR'} \{D, \rho_R(t)\}_+ + \sum_{R'} \gamma_{RR'} \mathcal{J}[\rho_{R'}(t)], \quad (67)$$

where D and \mathcal{J} follows from Eq. (6). In this case, the evolution of the configurational populations [Eq. (2)] strongly depend on the state of the system. In fact, here the configurational transitions may only occur when a photon emission happens. Thus, in general it is not possible to write a simple equation for their evolution. Only when $\{\gamma_{RR'}\} \ll \{\gamma_R\}$, a classical rate equation similar to Eq. (41) can be derived [31, 36].

1. Photon measurement operator

Here, the photon-measurement superoperator $\hat{\mathcal{M}}_{\text{ph}}|\rho\rangle = \hat{\mathcal{J}}_{\text{ph}}|\rho\rangle / \text{Tr}_S(1|\hat{\mathcal{J}}_{\text{ph}}|\rho\rangle)$, from Eq. (67), reads

$$\hat{\mathcal{M}}_{\text{ph}}|\rho\rangle = \frac{\sum_R |R\rangle \{\gamma_R \sigma \rho_R \sigma^\dagger + \sum_{R'} \gamma_{RR'} \sigma \rho_{R'} \sigma^\dagger\}}{\sum_{R''} \tilde{\gamma}_{R''} \text{Tr}_S[\sigma^\dagger \sigma \rho_{R''}]}, \quad (68)$$

where $|\rho\rangle = \sum_R |R\rangle \rho_R$, and we have defined the rate

$$\tilde{\gamma}_R \equiv \gamma_R + \sum_{R'} \gamma_{R'R}. \quad (69)$$

As in the previous case [Eq. (42)], Eq. (68) take into account all possible configurational paths that lead to a photon emission. The conditional evolution defined by the operator $\hat{\mathcal{D}} = \hat{\mathcal{L}} - \hat{\mathcal{J}}_{\text{ph}}$, expressed through the evolution of the unnormalized state $|\rho_t^u\rangle$ [Eq. (44)] reads

$$\frac{d\rho_R^u(t)}{dt} = \frac{-i}{\hbar} [H_R, \rho_R^u(t)] - \tilde{\gamma}_R \{D, \rho_R^u(t)\}_+. \quad (70)$$

Notice that in contrast with Eq. (45), here the conditional evolution is diagonal in the R -space.

2. Stochastic dynamics

The structure of the stochastic dynamics of the vectorial state $|\rho_t^{\text{st}}\rangle$, Eq. (34), is similar to that of the previous case. When a photon detection event happens it implies the transformation

$$|\rho_t^{\text{st}}\rangle \rightarrow \hat{\mathcal{M}}_{\text{ph}}|\rho_t^{\text{st}}\rangle = |-\rangle \langle -| \sum_R p_R^{\text{st}}(t) |R\rangle, \quad (71)$$

where the weights satisfies $\sum_R p_R^{\text{st}} = 1$. From Eq. (68), here they read

$$p_R^{\text{st}}(t) \equiv \frac{\gamma_R \langle + | \rho_R^{\text{st}}(t) | + \rangle + \sum_{R'} \gamma_{RR'} \langle + | \rho_{R'}^{\text{st}}(t) | + \rangle}{\sum_{R''} \tilde{\gamma}_{R''} \langle + | \rho_{R''}^{\text{st}}(t) | + \rangle}. \quad (72)$$

From Eq. (37) it is simple to demonstrate that Eqs. (48) and (49) are also valid in this case. Therefore, in each photon recording event the system collapse to its ground state while $p_R^{\text{st}}(t)$ define the posterior value of the configurational populations.

In the next figures we consider a fluorophore system whose evolution is defined by Eq. (67) and a two-dimensional configurational space, $R = A, B$. The Rabi frequencies [Eq. (4)] do not depend on the configurational states, $\Omega_R = \Omega$, and the spectral shifts [Eq. (5)] are null, $\delta\omega_R = 0$. Therefore, the bath states only affect the decay rates $\{\gamma_R\}$ of the system. The laser is in resonance with the system, i.e., $\omega_L = \omega_0$.

In Fig. 6(a) we show a realization of the upper population of the system $\langle + | \rho_S^{\text{st}}(t) | + \rangle$ [Eq. (37)]. The times of the photon emission events correspond to the collapse of the upper population to zero. Fig. 6(b) shows the realization of the configurational population of the bath

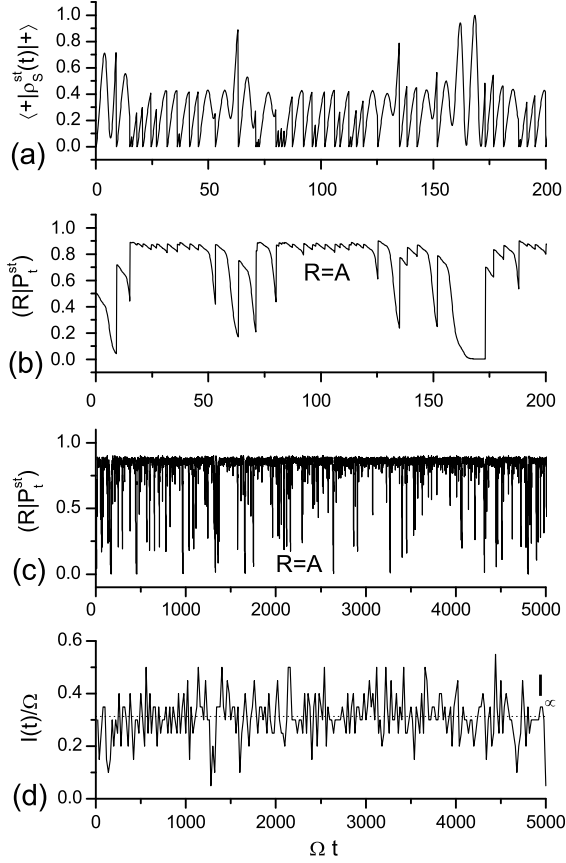


FIG. 6: Stochastic realizations of a fluorophore system defined by the evolution Eq. (67). The configurational space is two-dimensional, $R = A, B$. The parameters are $\Omega_R = \Omega$, $\delta\omega_R = 0$, $\gamma_A/\Omega = 1.8$, $\gamma_B/\Omega = 0.15$, $\gamma_{AB}/\Omega = 0.35$, $\gamma_{BA}/\Omega = 0.2$. The laser is in resonance with the system, i.e., $\omega_L = \omega_0$. (a) Realization of the upper population of the system $\langle + | \rho_S^{\text{st}}(t) | + \rangle$. (b)-(c) Realization of the configurational population of the bath $\langle R | P_t^{\text{st}} \rangle$, for $R = A$. (d) Intensity realization. I_∞ is defined by Eq. (73).

$\langle R | P_t^{\text{st}} \rangle$, for $R = A$ [Eq. (37)]. Due to the chosen parameter values, at any time it is not possible to predict with total certainty [$\langle R | P_t^{\text{st}} \rangle \approx 1$] the configurational state of the reservoir. This fact is evident from Fig. 6(c), where we plot $\langle R | P_t^{\text{st}} \rangle$ (for $R = A$) over a larger time interval. In Fig. 6(d), we plot the scattered intensity. Consistently with the behavior of $\langle R | P_t^{\text{st}} \rangle$, the intensity does not develop any dichotomic behavior. The intensity fluctuates around the value I_∞ defined by (see Eq. (55) in Ref. [31])

$$I_\infty = \sum_R \tilde{\gamma}_R \langle + | \rho_R^\infty | + \rangle, \quad (73)$$

where as before $\rho_R^\infty = \lim_{t \rightarrow \infty} \rho_R(t)$.

In Fig. 7(a) and (b) we plot the analytical solutions of the upper population $\langle + | \rho_S(t) | + \rangle$ and the configurational populations $\langle R | P_t \rangle$ that follows from Eq. (67) [and Eq. (2)]. The noisy curves correspond to an average over realizations like those shown in Fig. 6. Notice

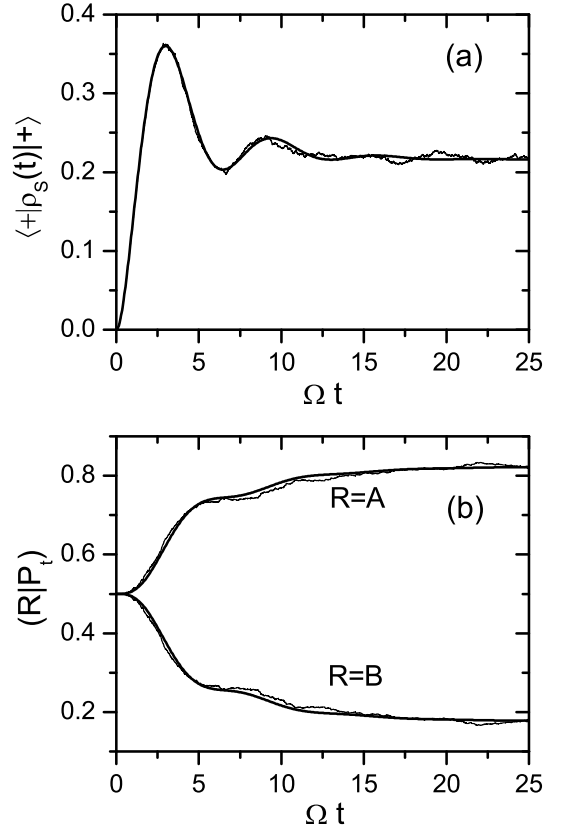


FIG. 7: Evolution of the upper population $\langle + | \rho_S(t) | + \rangle$ (a) and the configurational populations $\langle R | P_t \rangle = \text{Tr}_S[\langle R | \rho_t \rangle]$ (b) that follow from Eq. (67). The parameters are the same than in Fig. 6. The initial conditions are $\rho_S(0) = |-\rangle \langle -|$ and $\langle A | P_0 \rangle = \langle B | P_0 \rangle = 1/2$. The noisy curves follow from an average over the realizations shown in Fig. 6.

that here, the behavior of the configurational population strongly depart from an exponential one, indicating that their underlying dynamics is highly non-Markovian. The physical origin of this characteristic is the dependence of the configurational transitions on the system state.

3. Photon emission process

In this case it is also possible to define a stochastic waiting time distribution that parametrically depends on the configurational populations after a photon detection event, i.e., $w_{\text{st}}(t, t') = \text{Tr}_S[(1 | \hat{\mathcal{J}} e^{\hat{\mathcal{D}}(t-t')} \hat{\mathcal{M}}_{\text{ph}} | \rho_{t'}^{\text{st}} \rangle]$, Eq. (51). From Eqs. (68) and (71) we get

$$w_{\text{st}}(t, t') = \sum_{RR'} \tilde{\gamma}_R \langle + | e_{RR'}^{\hat{\mathcal{D}}(t-t')} | - \rangle \langle - | p_{R'}^{\text{st}}(t') | + \rangle, \quad (74)$$

where $p_{R'}^{\text{st}}(t')$ is given by Eq. (72). As the vectorial superoperator $\hat{\mathcal{D}}$ is diagonal [see Eq. (70)], this expression can be written as

$$w_{\text{st}}(t, t') = \sum_R \tilde{w}_R(t-t') p_R^{\text{st}}(t'), \quad (75)$$

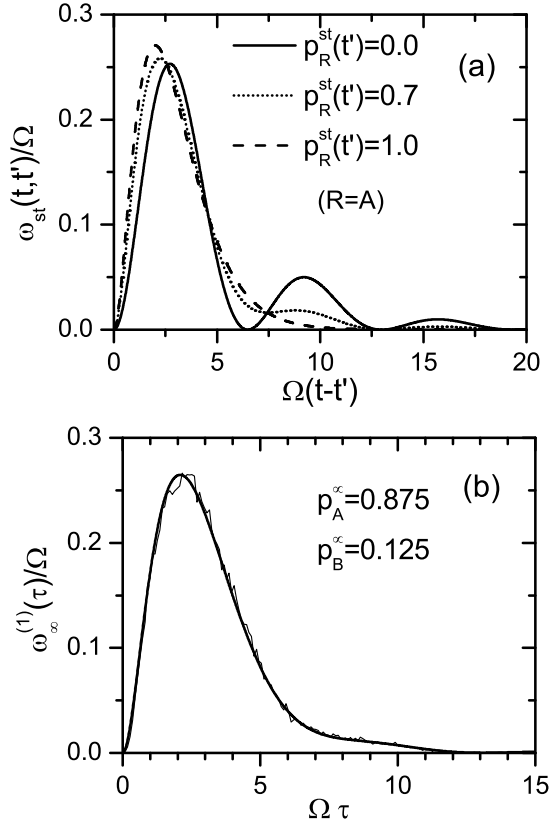


FIG. 8: (a) Plot of the waiting time distribution $w_{st}(t, t')$ [Eq. (75)] for different values of $p_R^{st}(t')$. We take the values $p_R^{st}(t') = 0$ (full line), 0.7 (dotted line), and 1 (dashed line), where $R = A$. (b) Stationary waiting time distribution [Eq. (76)]. The stationary weights [Eq. (77)] read $p_A^{\infty} = 0.875$ and $p_B^{\infty} = 0.125$. The noisy curve corresponds to the time average Eq. (10). The parameters are the same than in Fig. 6.

where $\tilde{w}_R(t)$ is defined by Eq. (63) after the replacement $\gamma_R \rightarrow \tilde{\gamma}_R$ [Eq. (69)]. While Eq. (59) is an approximation valid in the limit of slow environmental fluctuations, here Eq. (75) is valid independently of the values of any of the parameters that define the system evolution, Eq. (67).

In Fig. 8(a), we plot $w_{st}(t, t')$ (as a function of $t - t'$) for different values of the parameters $p_R^{st}(t')$. As in the previous case, $w_{st}(t, t')$ has a strong dependence on the values of the configurational populations $\{p_{R'}^{st}(t')\}$, implying strong departures from a renewal process. In fact, notice that depending on $p_{R'}^{st}(t')$, $w_{st}(t, t')$ may or not to develop oscillatory behaviors.

4. Stationary waiting time distributions

The first stationary waiting time distribution Eq. (10) from Eq. (32) can be written as $w_{\infty}^{(1)}(\tau) = \sum_{RR'} \tilde{\gamma}_R \langle + | e^{\tilde{\mathcal{D}}_R \tau} | - \rangle \langle - | p_R^{\infty} | + \rangle$. After using the defi-

nition of the conditional evolution Eq. (70), it follows

$$w_{\infty}^{(1)}(\tau) = \sum_R \tilde{w}_R(\tau) p_R^{\infty}, \quad (76)$$

where the weights p_R^{∞} are determined from the relation $\hat{\mathcal{M}}_{ph} |\rho_{\infty}\rangle = |-\rangle \langle - | \sum_R p_R^{\infty} | R \rangle$, delivering

$$p_R^{\infty} \equiv \frac{\gamma_R \langle + | \rho_R^{\infty} | + \rangle + \sum_{R'} \gamma_{RR'} \langle + | \rho_{R'}^{\infty} | + \rangle}{\sum_{R''} \tilde{\gamma}_{R''} \langle + | \rho_{R''}^{\infty} | + \rangle}. \quad (77)$$

In Fig. 8(b) we plot the analytical expression for $w_{\infty}^{(1)}(\tau)$ [Eq. (76)] joint with the numerical distribution (noisy curve) obtained as the probability distribution of the time intervals between successive photon emissions along a single trajectory, Eq. (10). The theoretical and numerical results match between them.

The second waiting time distribution $w_{\infty}^{(2)}(\tau_2, \tau_1)$ follows from Eq. (33). After some calculations we get

$$w_{\infty}^{(2)}(\tau_2, \tau_1) = \sum_R \left\{ \tilde{w}_R(\tau_2) q_R + \sum_{R'} \tilde{w}_{R'}(\tau_2) q_{R'R} \right\} \times \tilde{w}_R(\tau_1) p_R^{\infty}. \quad (78)$$

Here, we introduced the factors

$$q_R \equiv \frac{\gamma_R}{\tilde{\gamma}_R}, \quad q_{R'R} \equiv \frac{\gamma_{R'R}}{\tilde{\gamma}_R}, \quad (79)$$

which for any R satisfy the normalization $q_R + \sum_{R'} q_{R'R} = 1$.

The physical content of Eq. (78) can be read as follows. After a first photon emission [contribution $\tilde{w}_R(\tau_1) p_R^{\infty}$], the second one happens without a configurational transition with probability q_R , while with probability $q_{R'R}$ it is endowed with the configurational transition $R \rightarrow R'$. This interpretation is consistent with the results presented in Ref. [36] (see also Appendix A). On the other hand, while in general $w_{\infty}^{(2)}(\tau_2, \tau_1) \neq w_{\infty}^{(2)}(\tau_1, \tau_2)$, here for two-dimensional configurational spaces $w_{\infty}^{(2)}(\tau_2, \tau_1)$ is symmetric on its arguments.

In Fig. 9(a) we plot $w_{\infty}^{(2)}(\tau_2, \tau_1)$ [Eq. (78)] for different values of τ_1 . We also show the numerical distribution, Eq. (11). In Fig. 9(b) we plot the dimensionless parameter $\Lambda(\tau_2, \tau_1)$ [Eq. (12)] determined from Eqs. (76) and (78), for different values of τ_1 . In Fig. 10 we show its contour plot as well as that corresponding to $w_{\infty}^{(2)}(\tau_2, \tau_1)$. For small values of τ_2 and τ_1 , $\Lambda(\tau_2, \tau_1)$ is almost null, while for higher values of both times $\Lambda(\tau_2, \tau_1)$ reaches its maximal values.

We notice that the structure of $w_{\infty}^{(2)}(\tau_2, \tau_1)$ is very similar to that shown in Fig. 5. The same affirmation is valid for the corresponding $w_{\infty}^{(1)}(\tau)$, i.e., Fig. 3(b) and 8(b). Nevertheless, here $\Lambda(\tau_2, \tau_1)$ [Fig. 10] develops a much richer structure or dependence in τ_2 and τ_1 . The origin of this characteristic can be related with the behavior of the underlying photon-to-photon emission process. In fact, in the light assisted case $w_{st}(t, t')$ [Fig. 8(a)],

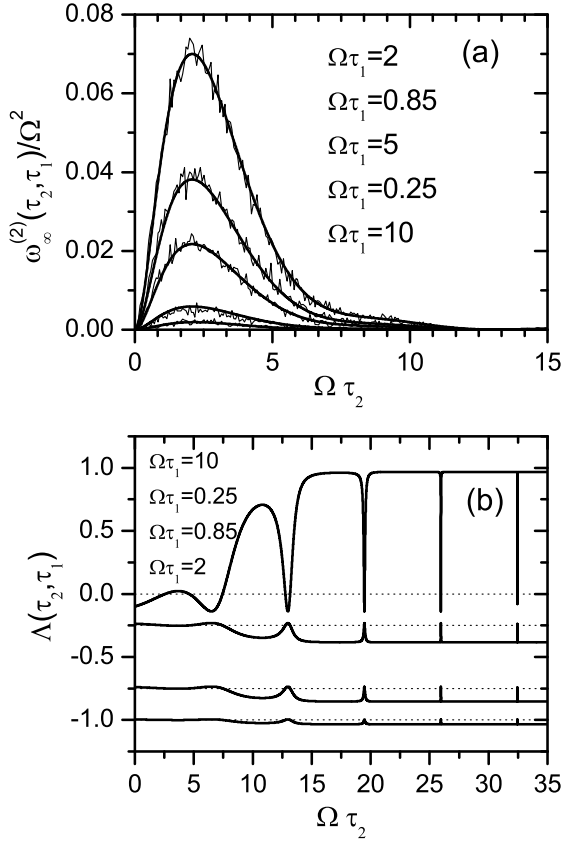


FIG. 9: (a) Stationary two-time waiting time distribution $w_{\infty}^{(2)}(\tau_2, \tau_1)$ [Eq. (78)] for different values of τ_1 . From top to bottom we take $\Omega\tau_1 = 2, 0.85, 5, 0.25$, and 10 . The noisy curves correspond to the time average Eq. (11). (b) Parameter $\Lambda(\tau_2, \tau_1)$ [Eq. (12)] determine from Eqs. (76) and (78), for different values of τ_1 . From top to bottom $\Omega\tau_1 = 10, 0.25, 0.85$, and 2 . For clarity, the curves corresponding to the last three values were shifted by $-0.25, -0.75$, and -1 respectively. The parameters are the same than in Fig. 6.

depending on the values of the parameter $p_R^{\text{st}}(t')$, may develop strong oscillatory behaviors, while in Fig. 3(a) the behaviors are almost monotonous. Independently of the underlying environmental dynamic, by increasing the external laser intensity the renewal departure measure $\Lambda(\tau_2, \tau_1)$ develops a richer structure.

When the radiation pattern develops a blinking phenomenon [31], i.e., for slow (light-assisted) environment fluctuations, $\{\gamma_{RR'}\} \ll \{\gamma_R\}$, Eq. (77) becomes

$$p_R^{\infty} \simeq \frac{\tilde{I}_R \tilde{P}_R^{\infty}}{\sum_{R'} \tilde{I}_{R'} \tilde{P}_{R'}^{\infty}}, \quad (80)$$

where \tilde{I}_R follows from Eq. (50) under the replacement $\gamma_R \rightarrow \tilde{\gamma}_R$ [Eq. (69)], and the probabilities \tilde{P}_R^{∞} are the stationary solution of a classical master equation obtained from Eq. (41) under the replacement $\phi_{RR'} \rightarrow \Gamma_{R'R} = q_{R'R} \tilde{I}_R$ (see Eqs. (81) and (82) in Ref. [31]). In the limit of fast environment fluctuations, $\{\gamma_{RR'}\} \gg \{\gamma_R\}$, the photon emission process becomes a renewal one.

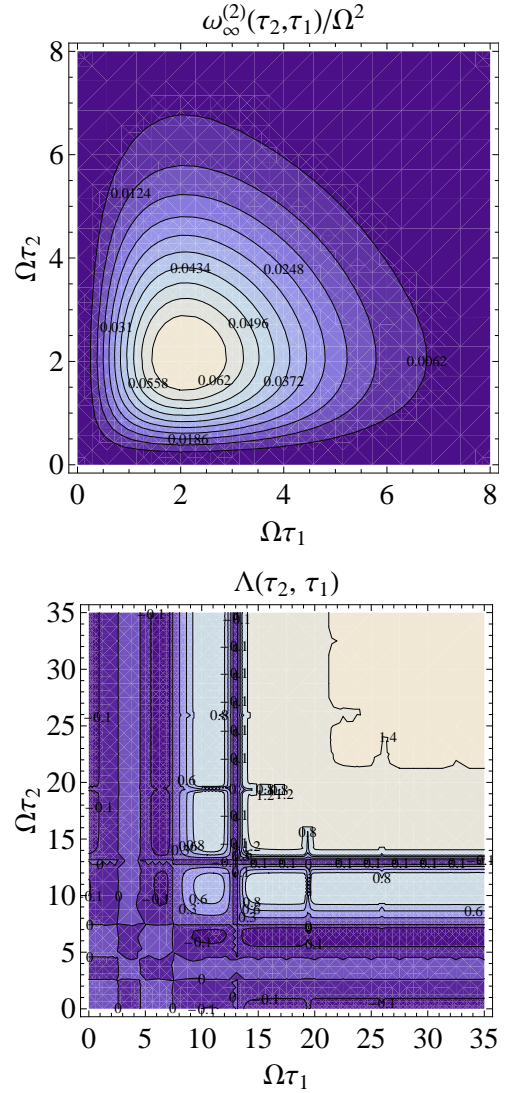


FIG. 10: Contour plot of $w_{\infty}^{(2)}(\tau_2, \tau_1)/\Omega^2$ [upper panel] and $\Lambda(\tau_2, \tau_1)$ [lower panel] corresponding to the plots of Fig. 9.

V. SUMMARY AND CONCLUSIONS

In this paper, we formulated a quantum-jump approach for describing the radiation patterns of single fluorescent systems coupled to complex fluctuating environments. Our results rely on a density matrix formulation of the problem. The master Eq. (3) take into account both the system dynamic as well as a width class of environment fluctuations.

The quantum-jump approach relies on a quantum measurement theory. Here, after introducing general measurement transformations acting on the system and the configurational bath space [Eq. (13)], the density matrix evolution was written as an average over measurement trajectories, Eq. (20). The weight of each trajectory is measured by its associated n -joint probability, Eq. (22). The hierarchy of these objects completely characterizes the statistical properties of the measurement processes.

Its functional form in an asymptotic time regime provides information about observables defined from a time average along a single measurement trajectory. Eqs. (32) define the stationary probability distribution for the time interval between consecutive measurement events, while Eq. (33) define the joint probability for two consecutive intervals. These two objects allow measuring the departure of the measurement process from a renewal one.

The decomposition of the density matrix evolution into a set of measurement trajectories leads to a stochastic representation of the system dynamics, Eq. (34). Each stochastic realization can be related with a particular measurement trajectory. Their structure allowed us to define how the measurement process occurs event-to-event. The waiting time distribution Eq. (39) defines the probability density for consecutive recording events. In contrast with a renewal process, it depends on the stochastic state of the system, property that breaks the renewal character of the measurement process. This dependence encodes the influence of the bath fluctuations.

The case when there exist only one measurement process, providing information about the photon emission events, was analyzed in detail. Independently of the underlying bath dynamics (and the measurement processes, see Appendix A) the photon-to-photon emission process is defined by a stochastic waiting time distribution that parametrically depends on the configurational bath populations. The analysis based on Eq. (40) allows to describing situations like spectral diffusion process, lifetime fluctuations and molecules diffusing in a solution. The stochastic waiting time distribution, Eq. (52), and the first and second stationary waiting time distributions, Eqs. (53) and (56) respectively, provides a deep characterization of the photon emission process. These general expressions assume a simple form when the environment fluctuations are much slower than the optical system transitions. In fact, in such a case those objects can be written as linear combinations of the waiting time distribution associated to a Markovian fluorescent system characterized by the parameters corresponding to each configurational state, Eqs. (59), (64), and (65). The case of light assisted process, Eq. (67), admits a similar description, Eqs. (75), (76), and (78).

The developed results provide an alternative theoretical tool for analyzing single fluorescent systems coupled to classically fluctuating environments. In fact, the explicit analytical characterization of statistical observables like the stationary waiting time distributions, Eqs. (10) and (11), and the renewal departure function, Eq. (12), may provide a power tool for deducing the underlying structure of complex nanoscopic reservoirs analyzed through fluorescence spectroscopy.

Acknowledgments

The author thanks fruitful discussions with R. Rebolledo, F. Petruccione, M. Orszag, and A. Barchielli

at the “30th Conference on Quantum Probability and Related Topics,” (2009) Santiago, Chile. This work was supported by CONICET, Argentina.

Appendix A: Measuring photon emissions and configurational transitions

In Section IV we characterized the quantum jump approach (for both self-environment fluctuations and light assisted processes) when the measurement action only gives information about the photon emission events. While that is the standard situation in SMS, the formalism developed in Section III allow us to analyze the case in which there exist extra measurement channels (apparatus) that give information about the configurational states of the reservoir. Besides its theoretical interest and potential applications, the following analysis also allows to understand some previous results [36].

Here, we assume that at any time one know which is the configurational state of the bath. Under this condition, the stochastic dynamic of $|\rho_t^{\text{st}}\rangle$ and $|P_t^{\text{st}}\rangle$ assume the structure

$$|\rho_t^{\text{st}}\rangle = \rho_S^{\text{st}}(t)|R_t^{\text{st}}\rangle, \quad |P_t^{\text{st}}\rangle = |R_t^{\text{st}}\rangle, \quad (\text{A1})$$

where $\text{Tr}_S[\rho_S^{\text{st}}(t)] = 1$, and R_t^{st} randomly change over the set of possible values $R = 1, 2, \dots, R_{\text{max}}$. Therefore, here the vectorial nature of $|\rho_t^{\text{st}}\rangle$ can be avoided. In fact, all relevant information is encoded in $\rho_S^{\text{st}}(t)$ and $\langle R|P_t^{\text{st}}\rangle = \delta_{RR_t^{\text{st}}}$ [see Eq. (37)]. While the underlying master equations are different, the results of Ref. [37] also rely on the previous assumption.

1. Self-fluctuating environments

First we analyze the case of self-fluctuating environments, Eq. (40). The parameter μ includes one term corresponding to the photon detector, $\mu = \text{ph}$, and $\mu = 1 \dots R_{\text{max}}$ terms that detect (measure) when a transition to a given conformational state R happens.

a. Measurement operators

The measurement operators [Eq. (13)] read

$$\hat{\mathcal{M}}_{\text{ph}}|\rho\rangle = \frac{\sum_R \gamma_R |R\rangle \sigma \rho_R \sigma^\dagger}{\sum_{R'} \gamma_{R'} \text{Tr}_S[\sigma^\dagger \sigma \rho_{R'}]}, \quad (\text{A2a})$$

$$\hat{\mathcal{M}}_R|\rho\rangle = \frac{|R\rangle \sum_{R'} \phi_{RR'} \rho_{R'}}{\sum_{R''} \phi_{RR''} \text{Tr}_S[\rho_{R''}]}, \quad (\text{A2b})$$

where $|\rho\rangle = \sum_R |R\rangle \rho_R$. The (unnormalized) conditional evolution [Eq. (44)] is diagonal in the R -space and reads

$$\frac{d\rho_R^{\text{u}}(t)}{dt} = \frac{-i}{\hbar} [H_R, \rho_R^{\text{u}}(t)] - \gamma_R \{D, \rho_R^{\text{u}}(t)\}_+ - \tilde{\phi}_R \rho_R^{\text{u}}(t), \quad (\text{A3})$$

where the rate $\tilde{\phi}_R$ is defined by

$$\tilde{\phi}_R \equiv \sum_{R'} \phi_{R'R}. \quad (\text{A4})$$

These definitions provide a splitting of Eq. (40) that allows to formulate the quantum-jump approach, Eq. (14). $\hat{\mathcal{M}}_{\text{ph}}$ corresponds to the transformation associated to a photon detection event. On the other hand, $\hat{\mathcal{M}}_R$ take in account all transitions $R' \rightarrow R$ that leave the bath in the configurational state R .

b. Stochastic dynamics

The measurement operators Eq. (A2) imply the transformations $[|\rho_t^{\text{st}}\rangle = \rho_S^{\text{st}}(t)|R_t^{\text{st}}\rangle]$

$$|\rho_t^{\text{st}}\rangle \rightarrow \hat{\mathcal{M}}_{\text{ph}}|\rho_t^{\text{st}}\rangle = |-\rangle\langle -| R_t^{\text{st}}, \quad (\text{A5a})$$

$$|\rho_t^{\text{st}}\rangle \rightarrow \hat{\mathcal{M}}_R|\rho_t^{\text{st}}\rangle = \rho_S^{\text{st}}(t)|R\rangle. \quad (\text{A5b})$$

The first transformation collapse the system to its ground state and does not affect the configurational state. The measurement operator $\hat{\mathcal{M}}_R$ leaves invariant the system state $\rho_S^{\text{st}}(t)$, while produces the configurational transition $|R_t^{\text{st}}\rangle \rightarrow |R\rangle$. On the other hand, notice that the dynamics between recording events, i.e., Eq. (A3), does not affect the configurational bath state.

From Eqs. (19) and (A2), it follows

$$F_{\text{ph}}[|\rho_t^{\text{st}}\rangle] = \gamma_{R_t^{\text{st}}} \langle +|\rho_S^{\text{st}}(t)|+\rangle, \quad (\text{A6a})$$

$$F_R[|\rho_t^{\text{st}}\rangle] = \phi_{RR_t^{\text{st}}}. \quad (\text{A6b})$$

Consistently with the classical evolution Eq. (41), the probability by unit of time for observing the configurational transition $|R_t^{\text{st}}\rangle \rightarrow |R\rangle$ [i.e., $\phi_{RR_t^{\text{st}}}$] is independent of the state of the system $\rho_S^{\text{st}}(t)$.

When a recording event happens, each transformation [Eqs. (A5)] must be selected in agreement with the transition probabilities $t_\mu(t)$, Eq. (36). They read

$$t_{\text{ph}}(t) = \frac{\gamma_{R_t^{\text{st}}} \langle +|\rho_S^{\text{st}}(t)|+\rangle}{\gamma_{R_t^{\text{st}}} \langle +|\rho_S^{\text{st}}(t)|+\rangle + \tilde{\phi}_{R_t^{\text{st}}}}, \quad (\text{A7a})$$

$$t_R(t) = \frac{\phi_{RR_t^{\text{st}}}}{\gamma_{R_t^{\text{st}}} \langle +|\rho_S^{\text{st}}(t)|+\rangle + \tilde{\phi}_{R_t^{\text{st}}}}, \quad (\text{A7b})$$

where $\tilde{\phi}_{R_t^{\text{st}}}$ follows from Eq. (A4). Notice that when a configurational transition happens, $|R_t^{\text{st}}\rangle \rightarrow |R\rangle$, the different possible final states $|R\rangle$ are chosen with probabilities $t_{R \leftarrow R_t^{\text{st}}} \equiv t_R(t) / \sum_{R'} t_{R'}(t) = \phi_{RR_t^{\text{st}}} / \tilde{\phi}_{R_t^{\text{st}}}$. This result can straightforwardly be read from the classical master equation (41).

In Fig. 11 we show the realizations associated to the measurement transformations Eq. (A5) and the evolution Eq. (40). They were build up by using the finite time step algorithm (Appendix D).

Fig. 11(a) shows a realization of the upper population of the system $\langle +|\rho_S^{\text{st}}(t)|+\rangle$ [Eq. (37)]. In contrast with

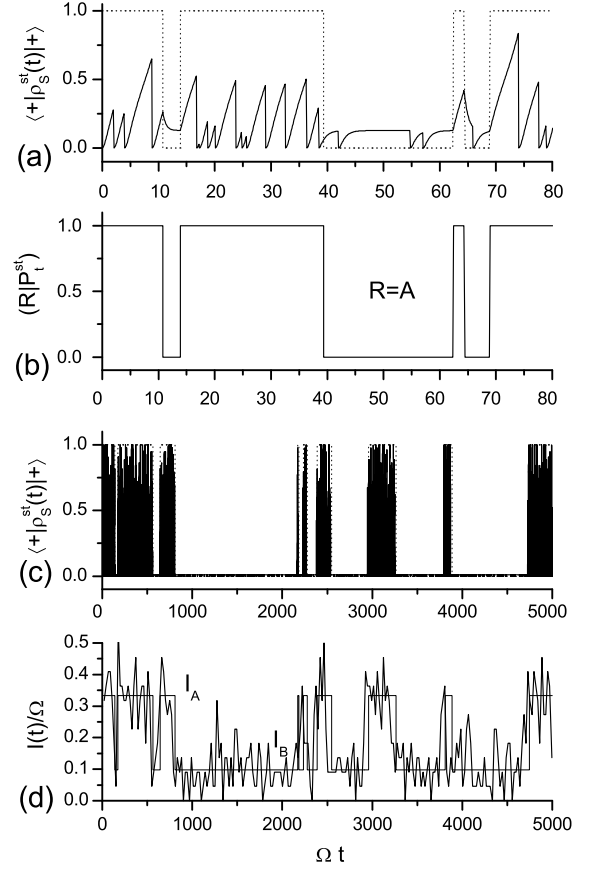


FIG. 11: Stochastic realizations of a fluorophore system defined by the evolution Eq. (40) and the measurement operators Eq. (A5). (a)-(c) Realization of the of the upper population of the system $\langle +|\rho_S^{\text{st}}(t)|+\rangle$. (b) Realization of the of the configurational population of the bath $(R|P_t^{\text{st}})$, for $R = A$. (d) Intensity realization. In (a) and (b), the parameters are $\Omega_R = \Omega$, $\delta\omega_R = 0$, $\gamma_A/\Omega = 1.5$, $\gamma_B/\Omega = 3$, $\phi_{AB}/\Omega = 0.03$, $\phi_{BA}/\Omega = 0.05$, and $\omega_L = \omega_0$. In (c) and (d), the parameters are the same than in Fig. 1.

Fig. 1, here each event may corresponds to a photon detection event, $\langle +|\rho_S^{\text{st}}(t)|+\rangle \rightarrow 0$ [Eq. (A5a)], or to a configurational transition (vertical dotted lines), Eq. (A5b). In these last events the upper population remains unaffected. In Fig. 11(b), we show the realization of $(R|P_t^{\text{st}})$, for $R = A$. In contrast with Fig. 1, here at all times we know with total certainty $[(R|P_t^{\text{st}}) = 1 \text{ or } 0]$ the configurational state of the bath.

In Fig. 11(c) and (d) we show the realization of $\langle +|\rho_S^{\text{st}}(t)|+\rangle$ and the scattered intensity $I(t)$. The parameters are the same than in Fig. 1. In (d), the telegraphic signal correspond to $\sum_R I_R(R|P_t^{\text{st}})$, where the intensities $\{I_R\}$ are defined by Eq. (50). This function assume the value I_R when the bath is in the configurational state R . The plot shows the direct correlation between the value of the intensity and the configurational bath state.

c. Recording process

Given that a recording event happens in the μ -detector at time t' , the waiting time distribution for the next event at time t is given by $w_{\text{st}}(t, t', \mu)$, Eq. (39). The event at time t is selected with probabilities $t_\mu(t)$, Eq. (A7). Here, $w_{\text{st}}(t, t', \mu)$ can be expressed in a shorter way through its associated survival probability, i.e., $w_{\text{st}}(t, t', \mu) = -(d/dt)P_0[t, t'; \hat{\mathcal{M}}_\mu|\rho_{t'}^{\text{st}}]$, Eq. (38). From Eqs. (A3) and (A5), we get

$$P_0[t, t'; \hat{\mathcal{M}}_{\text{ph}}|\rho_{t'}^{\text{st}}] = e^{-\tilde{\phi}_{R_{t'}^{\text{st}}}(t-t')} W_{R_{t'}^{\text{st}}}[t-t'; |-] \langle -|, \quad (\text{A8})$$

and for $R = 1, 2, \dots, R_{\text{max}}$,

$$P_0[t, t'; \hat{\mathcal{M}}_R|\rho_{t'}^{\text{st}}] = e^{-\tilde{\phi}_R(t-t')} W_R[t-t'; \rho_S^{\text{st}}(t')]. \quad (\text{A9})$$

Here, $W_R[t; \rho] \equiv \text{Tr}_S[\tilde{\rho}_R^{\text{u}}(t)]$, where $\tilde{\rho}_R^{\text{u}}(t)$ is the solution of the equation $(d/dt)\tilde{\rho}_R^{\text{u}}(t) = -(i/\hbar)[H_R, \tilde{\rho}_R^{\text{u}}(t)] - \gamma_R\{D, \tilde{\rho}_R^{\text{u}}(t)\}_+$, solved with the initial condition $\tilde{\rho}_R^{\text{u}}(0) = \rho$. Thus, $W_R[t; \rho]$ is the photon survival probability of a Markovian system that begins in the state ρ , and whose characteristic parameters are γ_R , ω_R , and Ω_R . In fact, the waiting time distribution Eq. (60) can also be written as $w_R(t) = -(d/dt)W_R[t; |-] \langle -|$.

The interpretation of the survival probabilities Eqs. (A8) and (A9) is very simple. The exponential factors take into account the probability of not having any configurational transition in the time interval (t', t) . On the other hand, the factors defined by $W_R[t; \rho]$ measure the probability of not having any photon emission in (t', t) . In Eq. (A9), $W_R[t-t'; \rho_S^{\text{st}}(t')]$ is the photon survival probability of a Markovian system (with parameters corresponding to the configurational state R) that begins in the (arbitrary) state $\rho_S^{\text{st}}(t')$. Consistently, in Eq. (A8) the factor $W_{R_{t'}^{\text{st}}}[t-t'; |-] \langle -|$ corresponds to the photon survival probability after happening a photon detection event at time t' , i.e., $\rho_S^{\text{st}}(t') = |-] \langle -|$. Hence, here the associated stochastic waiting time distributions $\{w_{\text{st}}(t, t', \mu)\}$ change when a configurational transition or when a photon recording event happen. Added to its dependence on the configurational state R , in contrast with the result of Section IV, $w_{\text{st}}(t, t', \mu)$ also may depend on the system state $\rho_S^{\text{st}}(t')$, i.e., its functional form depends parametrically on the matrix elements of $\rho_S^{\text{st}}(t')$.

We have checked that the stochastic dynamic of $|\rho_{t'}^{\text{st}}\rangle$ defined by Eqs. (A8) and (A9), like in Fig. 2, also recover the density matrix evolution defined by Eq. (40). As the dynamic of the configurational states is classical, the statistical properties of the photon-emission process remain the same. This fact is clearly seen by comparing Fig. 1(d) and Fig. 11(d). In both cases the intensity is characterized by the same telegraphic behavior.

2. Light assisted processes

Here we analyze the quantum-jump approach associated to Eq. (67) when both the photon emissions and the configurational transitions are measured, Eq. (A1).

a. Measurement operators

From Eq. (67) the measurement transformations read

$$\hat{\mathcal{M}}_{\text{ph}}|\rho\rangle = \frac{\sum_R \gamma_R |R\rangle \sigma \rho_R \sigma^\dagger}{\sum_{R'} \gamma_{R'} \text{Tr}_S[\sigma^\dagger \sigma \rho_{R'}]}, \quad (\text{A10a})$$

$$\hat{\mathcal{M}}_R|\rho\rangle = \frac{|R\rangle \sum_{R'} \gamma_{RR'} \sigma \rho_{R'} \sigma^\dagger}{\sum_{R''} \gamma_{RR''} \text{Tr}_S[\sigma^\dagger \sigma \rho_{R''}]}, \quad (\text{A10b})$$

$R \in (1, R_{\text{max}})$, while the conditional evolution here is also defined by Eq. (70).

b. Stochastic dynamics

The transformations Eq. (A10) imply the transformations $[[\rho_t^{\text{st}}] = \rho_S^{\text{st}}(t)|R_t^{\text{st}}]$

$$|\rho_t^{\text{st}}\rangle \rightarrow \hat{\mathcal{M}}_{\text{ph}}|\rho_t^{\text{st}}\rangle = |-] \langle -| |R_t^{\text{st}}\rangle, \quad (\text{A11a})$$

$$|\rho_t^{\text{st}}\rangle \rightarrow \hat{\mathcal{M}}_R|\rho_t^{\text{st}}\rangle = |-] \langle -| |R\rangle. \quad (\text{A11b})$$

While $\hat{\mathcal{M}}_{\text{ph}}$ collapse the system to its ground state and leaves invariant the configurational state, the superoperators $\hat{\mathcal{M}}_R$ produces both the system collapse and the configurational transition $R_t^{\text{st}} \rightarrow R$. Therefore, here any recording event (due to $\hat{\mathcal{M}}_{\text{ph}}$ or to $\hat{\mathcal{M}}_R$) implies a photon detection event.

The transformations defined by Eq. (A11) must to be selected in agreement with the transition probabilities $t_\mu(t)$, Eq. (36). From Eqs. (19) and (A10), we obtain

$$F_{\text{ph}}[[\rho_t^{\text{st}}]] = \gamma_{R_t^{\text{st}}} \langle + | \rho_S^{\text{st}}(t) | + \rangle, \quad (\text{A12a})$$

$$F_R[[\rho_t^{\text{st}}]] = \gamma_{RR_t^{\text{st}}} \langle + | \rho_S^{\text{st}}(t) | + \rangle. \quad (\text{A12b})$$

Then, the transition probabilities read

$$t_{\text{det}}(t) = \frac{\gamma_{R_t^{\text{st}}}}{\tilde{\gamma}_{R_t^{\text{st}}}}, \quad t_R(t) = \frac{\gamma_{RR_t^{\text{st}}}}{\tilde{\gamma}_{R_t^{\text{st}}}}. \quad (\text{A13})$$

Notice that these objects are independent of the state $\rho_S^{\text{st}}(t)$. Furthermore, they are stretched related with the definitions Eq. (79).

Fig. 12 shows the realizations associated to the measurement transformations Eq. (A11) and the evolution Eq. (67). The realizations were determined by using the finite time step algorithm (Appendix D). The parameters are the same than in Fig. 6.

Fig. 12(a) shows a realization of the upper population of the system $\langle + | \rho_S^{\text{st}}(t) | + \rangle$ [Eq. (37)]. The vertical dotted lines correspond to the time where the configurational transitions happen. In Fig. 12(b), we show the

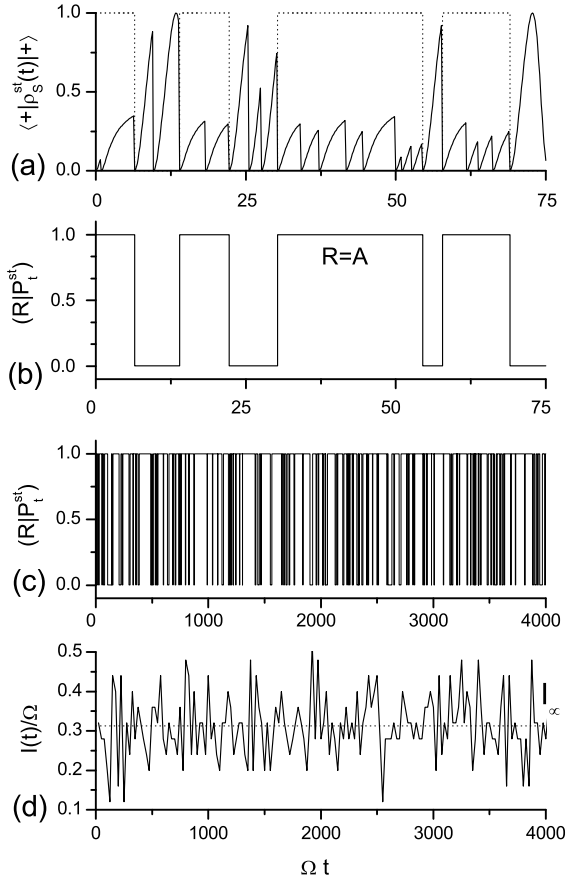


FIG. 12: Stochastic realizations of a fluorophore system defined by the evolution Eq. (67) and the measurement transformations Eq. (A11). (a) Realization of the of the upper population of the system $\langle +|\rho_S^{\text{st}}(t)|+ \rangle$. (b)-(c) Realization of the of the configurational population of the bath $(R|P_t^{\text{st}})$, for $R = A$. (d) Intensity realization. The parameters are the same than in Fig. 6.

realization of the configurational population $(A|P_t^{\text{st}})$. In contrast with Fig. 11(a) and (b), we notice that here the configurational transitions are always endowed with a photon emission. Furthermore, at all times the configurational state of the bath is known with total certainty $[(R|P_t^{\text{st}}) = 1 \text{ or } 0]$ [compare with Fig. 6(b) and (c)].

Fig. 12(c) shows $(A|P_t^{\text{st}})$ over a larger time scale while in Fig. 12(d) we show the scattered intensity $I(t)$. As expected, the intensity realization is similar to that shown in Fig. 6(d).

c. Recording process

The stochastic waiting time distributions Eq. (39), from Eqs. (70) and (A11), here read

$$w_{\text{st}}(t, t', \text{ph}) = \tilde{w}_{R_t^{\text{st}}}(t - t'), \quad (\text{A14a})$$

$$w_{\text{st}}(t, t', R) = \tilde{w}_R(t - t'), \quad (\text{A14b})$$

where $\tilde{w}_R(t)$ follows from Eq. (63) after the replacement $\gamma_R \rightarrow \tilde{\gamma}_R$ [Eq. (69)], i.e., they are the waiting time distribution of a Markovian fluorescent system with decay rate $\tilde{\gamma}_R$, detuning δ_R , and Rabi frequency Ω_R .

The expressions written in Eq. (A14) only differ in their sub-index (R_t^{st} or R). After a recording event, the indexes must be chosen with probabilities (A13). Therefore, $w_{\text{st}}(t, t', \mu)$ during successive photon recording events is randomly selected over the set of functions $\{\tilde{w}_R(t)\}$. This result recovers the analysis developed in Ref. [36]. For the example shown in Fig. (12), the two functions $\tilde{w}_A(t - t')$ and $\tilde{w}_B(t - t')$ can be read from Fig. 8(a) by taking $p_A^{\text{st}}(t') = 1$ and $p_A^{\text{st}}(t') = 0$ respectively. On the other hand, from Eqs. (A13) and (A14), one can deduce that here the stationary photon waiting time distributions are also defined by Eqs. (76) and (78).

Appendix B: Stationary n-joint probabilities

The probabilities Eq. (22) define the ensemble statistic of the measurement process. They depend on the initial condition $|\rho_0\rangle$. The statistical information that can be obtained from a time average along a single realization can be obtained from the stationary n -joint probabilities $P_n^\infty[\tau, \{\tau_i\}_1^n, \{\mu_i\}_1^n]$. They define the events statistics after happening an infinite number of measurements events and that an infinite time elapsed since the initial condition,

$$P_n^\infty[\tau, \{\tau_i\}_1^n, \{\mu_i\}_1^n] \equiv \lim_{N \rightarrow \infty} \lim_{t_N \rightarrow \infty} \int_0^{t_N} dt_{N-1} \cdots \int_0^{t_2} dt_1 \sum_{\nu_N \cdots \nu_1} P_{n+N}[t, \{t_i\}_1^{n+N}, \{\nu_i\}_1^{n+N}].$$

The new time variables are defined as $\tau \equiv t - t_N$, $\tau_i \equiv t_{i+N} - t_N$. The measurement apparatus indexes are $\mu_i = \nu_{i+N}$. By working in a Laplace domain, from Eq. (27) it is possible to obtain

$$P_n^\infty[\tau, \{\tau_i\}_1^n, \{\mu_i\}_1^n] = \text{Tr}_S[(1|e^{\hat{\mathcal{D}}(\tau - \tau_n)} \hat{\mathcal{J}}_{\mu_n} \cdots \hat{\mathcal{J}}_{\mu_2} e^{\hat{\mathcal{D}}(\tau_2 - \tau_1)} \times \hat{\mathcal{J}}_{\mu_1} e^{\hat{\mathcal{D}}\tau_1} \hat{\mathcal{M}}|\rho_\infty)] F_\infty. \quad (\text{B1})$$

Here the measurement operator $\hat{\mathcal{M}}$ is defined by Eq. (31), and the constant F_∞ reads

$$F_\infty \equiv \sum_\mu F_\mu[|\rho_\infty\rangle] = \text{Tr}_S[(1|\hat{\mathcal{J}}|\rho_\infty)], \quad (\text{B2})$$

where F_μ follows from Eq. (19) and we used Eq. (31), $\hat{\mathcal{J}} \equiv \sum_\mu \hat{\mathcal{J}}_\mu$. The stationary state $|\rho_\infty\rangle$ is defined by Eq. (30).

From Eq. (B1), by performing the inverse calculations steps than in the derivation of Eq. (27), it follows

$$P_n^\infty[\tau, \{\tau_i\}_1^n, \{\mu_i\}_1^n] = P_0[\tau, \tau_n; \hat{\mathcal{M}}_{\mu_n} |\rho_{\tau_n}]\prod_{j=2}^n w_{\mu_j}[\tau_j, \tau_{j-1}; \hat{\mathcal{M}}_{\mu_{j-1}} |\rho_{\tau_{j-1}}] \times w_{\mu_1}[\tau_1, 0; \hat{\mathcal{M}}|\rho_\infty] F_\infty. \quad (\text{B3})$$

The auxiliary states read $|\rho_{\tau_{i+1}}\rangle = \hat{T}(\tau_{i+1}, \tau_i) \hat{\mathcal{M}}_{\mu_i} |\rho_{\tau_i}\rangle$, where $|\rho_{\tau_1}\rangle = \hat{T}(\tau_1, 0) \hat{\mathcal{M}} |\rho_\infty\rangle$.

The interpretation (and structure) of Eq. (B3) is similar to that of Eq. (22). Nevertheless, here the factor F_∞ takes into account the probability by unit of time of having an arbitrary detection event in the long time regime. The associated measurement operator is $\hat{\mathcal{M}}$, Eq. (31). Furthermore, in contrast to Eq. (22), the first contribution (waiting time distribution) in Eq. (B3) is defined with the state $\hat{\mathcal{M}}|\rho_\infty\rangle$, i.e., the state after an arbitrary detection happening in the stationary regime. From Eqs. (B3) and (B1), the expressions Eqs. (32) and (33) follows straightforwardly after replacing $\tau_1 \rightarrow \tau_1$, and $\tau_2 \rightarrow \tau_1 + \tau_2$. In fact, the variables $\{\tau_i\}_1^n$ of the stationary waiting time distributions $w_\infty^{(n)}[\{\tau_i\}_1^n, \{\mu_i\}_1^n]$ denotes the time interval between consecutive recording events.

Appendix C: Averaging over realizations

Here, we demonstrate that the deterministic evolution Eq. (14) is recovered after averaging Eq. (34) over realizations of the Poisson processes N_t^μ .

First, by using that $(dN_t^\mu)^k = dN_t^\mu$ and the property $dN_t^\mu dN_t^{\mu'} = \delta_{\mu\mu'} dN_t^\mu$, it is possible to get the relation [3]

$$\overline{\Xi(\{N_t^\mu\}) dN_t^\mu} = \overline{\Xi(\{N_t^\mu\}) \text{Tr}_S[(1|\hat{\mathcal{J}}_\mu|\rho_t^{\text{st}})]} dt, \quad (\text{C1})$$

where $\Xi(\{N_t^\mu\})$ is an arbitrary function of the Poisson processes $\{N_t^\mu\}$. This equality can be immediately deduced by introducing a series expansion of Ξ . Now, we split the average of Eq. (34) as

$$\left. \frac{d}{dt} |\rho_t\rangle \right|_{\hat{\mathcal{D}}} = \left. \frac{d}{dt} |\rho_t\rangle \right|_{\hat{\mathcal{M}}} + \left. \frac{d}{dt} |\rho_t\rangle \right|_{\hat{\mathcal{M}}}, \quad (\text{C2})$$

where the first contribution is associated to the conditional deterministic dynamics and the second one with the disruptive measurement changes. Then, trivially it follows

$$\left. \frac{d}{dt} |\rho_t\rangle \right|_{\hat{\mathcal{D}}} = \hat{\mathcal{D}}|\rho_t\rangle - \overline{\text{Tr}_S[(1|\hat{\mathcal{D}}|\rho_t^{\text{st}})]|\rho_t^{\text{st}})}. \quad (\text{C3})$$

On the other hand, by using the definition Eq. (13) and the relation Eq. (C1), we get

$$\left. \frac{d}{dt} |\rho_t\rangle \right|_{\hat{\mathcal{M}}} = \hat{\mathcal{J}}_\mu |\rho_t\rangle - \sum_\mu \overline{\text{Tr}_S[(1|\hat{\mathcal{J}}_\mu|\rho_t^{\text{st}})]|\rho_t^{\text{st}})}. \quad (\text{C4})$$

After introducing the relation $\text{Tr}_S[(1|\hat{\mathcal{D}}|\bullet)] = -\sum_\mu \text{Tr}_S[(1|\hat{\mathcal{J}}_\mu|\bullet)]$ in Eqs. (C3) and (C4), the evolution Eq. (14) follows straightforwardly.

Appendix D: Algorithms associated to the stochastic evolution

Two different algorithms allow to build up the realizations associated to the stochastic evolution Eq. (34).

1. Infinitesimal time step algorithm

In the first algorithm, the stochastic state $|\rho_{t+\Delta t}^{\text{st}}\rangle$ is obtained from $|\rho_t^{\text{st}}\rangle$, where Δt is the time discretization step. By defining the quantity

$$F(t) \equiv \sum_\mu F_\mu[|\rho_t^{\text{st}}\rangle] = \sum_\mu \text{Tr}_S[(1|\hat{\mathcal{J}}_\mu|\rho_t^{\text{st}})], \quad (\text{D1})$$

the probability ΔP of having a measurement event is defined by $\Delta P = \Delta t F(t)$. Then, a random number r in $(0, 1)$ is generated and compared with ΔP . If $r > \Delta P$, no recording event happens, so the vectorial state evolves deterministically as [Eq. (17)]

$$|\rho_{t+\Delta t}^{\text{st}}\rangle = \hat{T}(t+\Delta t, t)|\rho_t^{\text{st}}\rangle \simeq \frac{(1 + \hat{\mathcal{D}}\Delta t)|\rho_t^{\text{st}}\rangle}{1 + \text{Tr}_S[(1|\hat{\mathcal{D}}\Delta t|\rho_t^{\text{st}})]}. \quad (\text{D2})$$

If $r < \Delta P$, there is measurement event. Then, the system state at $t + \Delta t$ is defined by [Eq. (13)]

$$|\rho_{t+\Delta t}^{\text{st}}\rangle = \hat{\mathcal{M}}_\mu |\rho_t^{\text{st}}\rangle = \frac{\hat{\mathcal{J}}_\mu |\rho_t^{\text{st}}\rangle}{\text{Tr}_S[(1|\hat{\mathcal{J}}_\mu|\rho_t^{\text{st}})]}. \quad (\text{D3})$$

Here, the index μ is chosen with probability $t_\mu(t)$, Eq. (36). Due to the relation $F_\mu[|\rho_t\rangle] = t_\mu(t)F(t)$, the generated realizations satisfy Eq. (34).

2. Finite time step algorithm

An alternative and more efficient algorithm can be defined by using the survival probability Eq. (18) [see also Eq. (38)]. Given that the state of the system after a measurement at time t_i is given by $\hat{\mathcal{M}}_{\mu_i} |\rho_{t_i}^{\text{st}}\rangle$, the time t_{i+1} of the next event is obtained from the equation

$$P_0[t_{i+1}, t_i; |\rho_{t_i}^{\text{st}}\rangle] = \text{Tr}_S[(1|e^{\hat{\mathcal{D}}(t_{i+1}-t_i)} \hat{\mathcal{M}}_{\mu_i} |\rho_{t_i}^{\text{st}}\rangle)] = r, \quad (\text{D4})$$

where as before r is a random number in the interval $(0, 1)$. For $t \in (t_{i+1}, t_i)$, the stochastic state evolves deterministically as [Eq. (17)]

$$|\rho_t^{\text{st}}\rangle = \hat{T}(t, t_i) \hat{\mathcal{M}}_{\mu_i} |\rho_{t_i}^{\text{st}}\rangle = \frac{e^{\hat{\mathcal{D}}(t-t_i)} \hat{\mathcal{M}}_{\mu_i} |\rho_{t_i}^{\text{st}}\rangle}{\text{Tr}_S[(1|e^{\hat{\mathcal{D}}(t-t_i)} \hat{\mathcal{M}}_{\mu_i} |\rho_{t_i}^{\text{st}}\rangle)]}. \quad (\text{D5})$$

At time $t = t_{i+1}$, an index μ_{i+1} is chosen with probability $\{t_\mu(t_{i+1})\}$, Eq. (36), and then the sudden transformation

$$|\rho_{t_{i+1}}^{\text{st}}\rangle \rightarrow \hat{\mathcal{M}}_{\mu_{i+1}} |\rho_{t_{i+1}}^{\text{st}}\rangle = \frac{\hat{\mathcal{J}}_{\mu_{i+1}} |\rho_{t_{i+1}}^{\text{st}}\rangle}{\text{Tr}_S[(1|\hat{\mathcal{J}}_{\mu_{i+1}}|\rho_{t_{i+1}}^{\text{st}})]}, \quad (\text{D6})$$

is applied. The first event follows from Eq. (D4) with $\hat{\mathcal{M}}_{\mu_i} |\rho_{t_i}^{\text{st}}\rangle \rightarrow |\rho_0^{\text{st}}\rangle$. The realizations generated with this algorithm are also consistent with the evolution Eq. (34).

-
- [1] H.J. Carmichael, *An Open Systems Approach to Quantum Optics*, Lecture Notes in Physics, Vol. M18 (Springer, Berlin, 1993).
- [2] M.B. Plenio and P.L. Knight, *Rev. Mod. Phys.* **70**, 101 (1998).
- [3] H.P. Breuer and F. Petruccione, *The theory of open quantum systems*, Oxford University press (2002).
- [4] P. Zoller, M. Marte, and D.F. Walls, *Phys. Rev. A* **35**, 198 (1987).
- [5] H.J. Carmichael, S. Singh, R. Vyas, and P.R. Rice, *Phys. Rev. A* **39**, 1200 (1989).
- [6] J. Dalibard, Y. Castin, and K. Molmer, *Phys. Rev. Lett.* **68**, 580 (1992).
- [7] R. Blatt and P. Zoller, *Eur. J. Phys.* **9**, 250 (1988).
- [8] G.C. Hegerfeldt and M.B. Plenio, *Quantum Opt.* **6**, 15 (1994).
- [9] G.C. Hegerfeldt and T.S. Wilser, in *Classical and Quantum Systems*, Proceedings of the Second International Wigner Symposium, July 1991, edited by H.D. Doebner, W. Scherer, and F. Schroeck (World Scientific, Singapore, 1992), p. 104.
- [10] G.C. Hegerfeldt, *Phys. Rev. A* **47**, 449 (1993); G.C. Hegerfeldt and D.G. Sondermann, *Quantum Semiclass. Opt.* **8**, 121 (1996).
- [11] A. Beige and G.C. Hegerfeldt, *Phys. Rev. A* **59**, 2385 (1999).
- [12] E. Barkai, Y. Jung, and R. Silbey, *Annu. Rev. Phys. Chem.* **55**, 457 (2004).
- [13] M. Lippitz, F. Kulzer, and M. Orrit, *Chem. Phys. Chem.* **6**, 770 (2005).
- [14] Y. Jung, E. Barkai, and R.J. Silbey, *J. Chem. Phys.* **117**, 10980 (2002).
- [15] R. Verberk and M. Orrit, *J. Chem. Phys.* **119**, 2214 (2003).
- [16] V. Bargesov, V. Chernyak, and S. Mukamel, *J. Chem. Phys.* **116**, 4240 (2002).
- [17] E. Barkai, Y. Jung, and R. Silbey, *Phys. Rev. Lett.* **87**, 207403 (2001).
- [18] G.C. Hegerfeldt and D. Seidel, *J. Chem. Phys.* **118**, 7741 (2003).
- [19] J. Wang and P. Wolynes, *Phys. Rev. Lett.* **74**, 4317 (1995).
- [20] F.L. Brown, *Phys. Rev. Lett.* **90**, 028302 (2003).
- [21] G.K. Schenter, H.P. Lu, and X.S. Xie, *J. Phys. Chem A* **103**, 10477 (1999).
- [22] V. Chernyak, M. Schultz, and S. Mukamel, *J. Chem. Phys.* **111**, 7416 (1999).
- [23] F. Sanda and S. Mukamel, *Phys. Rev. A* **71**, 033807 (2005).
- [24] H. Yang and X. Sunney Xie, *J. Chem. Phys.* **117**, 10965 (2002).
- [25] I.S. Osad'ko and V.V. Fedyanin, *J. Chem. Phys.* **130**, 064904 (2009); I.S. Osad'ko, *J. Chem. Phys.* **131**, 185101 (2009).
- [26] Y. Zheng and F.L. Brown, *Phys. Rev. Lett.* **90**, 238305 (2003).
- [27] Y. Zheng and F.L.H. Brown, *J. Chem. Phys.* **119**, 11814 (2003).
- [28] Y. Zheng and F.L.H. Brown, *J. Chem. Phys.* **121**, 3238 (2004).
- [29] Y. He and E. Barkai, *Phys. Rev. Lett.* **93**, 068302 (2004).
- [30] Y. He and E. Barkai, *J. Chem. Phys.* **122**, 184703 (2005).
- [31] A.A. Budini, *Phys. Rev. A* **79**, 043804 (2009).
- [32] A.A. Budini, *Phys. Rev. A* **74**, 053815 (2006); *Phys. Rev. E* **72**, 056106 (2005); A.A. Budini and H. Schomerus, *J. Phys. A* **38**, 9251, (2005); H.P. Breuer, *Phys. Rev. A* **75**, 022103 (2007).
- [33] F. Caycedo, F.J. Rodriguez, and G. Zumofen, *Phys. Rev. A* **78**, 053813 (2008).
- [34] A.A. Budini, *Phys. Rev. A* **73**, 061802(R) (2006); *J. Chem. Phys.* **126**, 054101 (2007).
- [35] A.A. Budini, *J. Phys. B* **40**, 2671 (2007).
- [36] A.A. Budini, *Phys. Rev. A* **76**, 023825 (2007).
- [37] M. Moodley and F. Petruccione, *Phys. Rev. A* **79**, 042103 (2009); X.L.Huang, H.Y. Sun, and X.X. Yi, *Phys. Rev. E* **78**, 041107 (2008).
- [38] N.G. van Kampen, *Stochastic Processes in Physics and Chemistry*, (Sec. Ed., North-Holland, Amsterdam, 1992), [see Chap. XVII Sect. 7, Internal noise].
- [39] In the context of Ref. [31], each vector $|R\rangle$ can be associated to a projector $|R\rangle\langle R|$, where the states $\{|R\rangle\}_{R=1}^{R_{\max}}$ define the effective configurational Hilbert space.
- [40] M. Tsang, *Phys. Rev. Lett.* **102**, 250403 (2009).